



**POWER SCINTILLATION FOR SUPER LORENTZ GAUSSIAN BEAM  
EVALUATION USING THE RANDOM PHASE SCREEN METHOD**

**HUSSEIN THARY KHAMEES AL-GHRAIRI**

**FEBRUARY 2018**

**POWER SCINTILLATION FOR SUPER LORENTZ GAUSSIAN BEAM  
EVALUATION USING THE RANDOM PHASE SCREEN METHOD**

**A THESIS SUBMITTED TO  
THE GRADUATE SCHOOL OF NATURAL AND APPLIED  
SCIENCES OF  
ÇANKAYA UNIVERSITY**

**BY  
HUSSEIN THARY KHAMEES AL-GHRAIRI**

**IN PARTIAL FULFILLMENT OF THE REQUIREMENTS FOR THE  
DEGREE OF**

**DOCTOR OF PHILOSOPHY**

**IN**

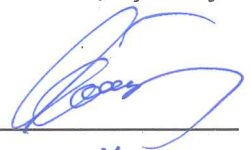
**THE DEPARTMENT OF  
ELECTRONIC AND COMMUNICATION ENGINEERING**

**FEBRUARY 2018**

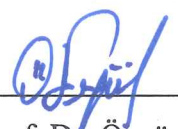
**Title of Thesis: Power Scintillation for Super Lorentz Gaussian Beam  
Evaluation Using the Random Phase Screen Method**

Submitted by **HUSSEIN THARY KHAMEES AL-GHRAIRI**


Approval of the Graduate School of Natural and Applied Sciences, Çankaya University.

  
\_\_\_\_\_  
Prof. Dr. Can COĞUN  
Director

I certify that this thesis satisfies all the requirements as a thesis for the degree of Doctor of Science.

  
\_\_\_\_\_  
Asst. Prof. Dr. Özgür ERGÜL  
*Acting* Head of Department

This is to certify that we have read this thesis and that in our opinion it is fully adequate, in scope and quality, as a thesis for the degree of Doctor of Science.

  
\_\_\_\_\_  
Asst. Prof. Dr. Serap Altay Arpali  
Supervisor

**Examination Date: 08.02.2018**

**Examining Committee Members**


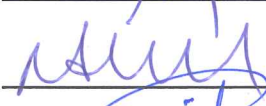


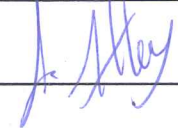
Prof. Dr. Halil Tanyer Eyyuboğlu (Çankaya Univ.)

Assoc. Prof. Dr. Nursel Akçam (Gazi Univ.)

Assoc. Prof. Dr. İsa Navruz (Ankara Univ.)

Asst. Prof. Dr. Barbaros Preveze (Çankaya Univ.)

Asst. Prof. Dr. Serap Altay ARPALI (Çankaya Univ.)

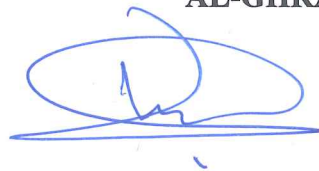
  
\_\_\_\_\_  
  
\_\_\_\_\_  
  
\_\_\_\_\_  
  
\_\_\_\_\_  
  
\_\_\_\_\_

## STATEMENT OF NON-PLAGIARISM PAGE

I hereby declare that all information in this document has been obtained and presented in accordance with academic rules and ethical conduct. I also declare that, as required by these rules and conduct, I have fully cited and referenced all material and results that are not original to this work.

Name-Surname : **HUSSEIN THARY KHAMEES  
AL-GHRAIRI**

Signature :

A handwritten signature in blue ink, consisting of a large, stylized loop followed by a horizontal line.

Date : 08.02.2018

## **ABSTRACT**

### **POWER SCINTILLATION FOR SUPER LORENTZ GAUSSIAN BEAM EVALUATION USING THE RANDOM PHASE SCREEN METHOD**

**HUSSEIN THARY KHAMEES AL-GHRAIRI**

Ph.D., Department of Electronic and Communication Engineering

Supervisor: Assist. Prof. Dr. Serap Altay Arpali

FEBRUARY 2018, 57 pages

In this thesis, the power scintillation of Super Lorentz Gaussian (SLG) beams is investigated. The behavior of the SLG beam in moderately turbulent and weakly turbulent atmospheres is analyzed numerically using the random phase screen method. The source size and wavelength variation for the power averaged scintillation index is observed by comparing wavelength variations for the point-like scintillation index and power scintillation index. From the numerical outputs, we observed that although the point-like scintillation index decreases with a smaller wavelength value, the power scintillation index is nearly the same for different wavelengths. Numerical results show that the power scintillation index decreases with an increasing source size, such as the point-like scintillation index. Depending on all propagation parameters, the power scintillation index of the SLG beam is smaller than the point-like scintillation index of the SLG beam. Additionally, from the average receiver intensity with different beam order, we noticed that the shape of the beam intensity expands with larger propagation distance. The amplitude of the SLG beam intensity decreases with larger propagation distance. In the receiver plane, the average intensity profile of the Super Lorentz Gaussian beam is described in two and three dimensions. Several different source sizes and wavelengths of the receiver intensity are studied and we have computed that the average receiver intensity

decreases at larger propagation distances. In this work, MATLAB codes are used to calculate the scintillation index and average intensity. Furthermore, to check the outputs, the scintillation index of the lowest order of the SLG beam (Gaussian beam) and the Gaussian beam of the scintillation index in the literature are compared under different parameters of turbulence.

**Keywords:** Aperture Averaging Scintillation, SLG, Point-like Scintillation, Random Phase Screen Method.



## ÖZ

### POWER SCINTILLATION FOR SUPER LORENTZ GAUSSIAN BEAM EVALUATION USING THE RANDOM PHASE SCREEN METHOD

**HUSSEIN THARY KHAMEES AL-GHRAIRI**

Doktora, Elektronik ve Haberleşme Mühendisliği Anabilim Dalı

Tez Yöneticisi: Yrd. Doç. Dr. Serap Altay Arpali

Şubat 2018, 57 sayfa

Bu tezde, Süper Lorentz Gauss (SLG) ışık hüzmelerinin belirli bir alıcı açıklık yarıçapı için ortalama optik güç pırladama indeksi incelenmiştir. Orta dereceli türbülanslı ve zayıf dereceli türbülanslı atmosferde SLG ışık hüzmesinin davranışı rastgele fazlı pencere yöntemi kullanılarak nümerik olarak analiz edilmiştir. Ortalama güç pırladama indeksi için kaynak boyutu ve dalga boyu değişimi gözlemlenmiştir. Buna ilaveten alıcı düzleminin merkez noktasında pırladama indeksi ile güç pırladama indeksi dalga boyu değişimlerine göre karşılaştırılmıştır. Nokta-pırladama indeksi, daha küçük dalga boyu değerleri ile azalmasına rağmen, güç pırladama indeksi farklı dalga boylarında hemen hemen aynıdır. Sayısal sonuçlara göre, güç pırladama indeksinin de nokta-pırladama indeksi gibi, artan kaynak boyutları ile azaldığı gözlemlenmiştir. Tüm yayılma parametrelerine bağlı olarak alınan sonuçlara göre, SLG ışık hüzmesinin güç pırladama indeksi, SLG ışık hüzmesinin nokta-pırladama indeksinden daha küçüktür. Ayrıca, alıcı düzleminde ortalama ışık şiddeti yoğunluğu profilleri, farklı yayılım mesafesi için çizdirilmiştir. Alınan sonuçlara göre artan mesafelerde ışık şiddetinin azaldığı ve genişlediği gözlemlenmiştir. Alıcı düzleminde, SLG ışık hüzmesinin ortalama ışık şiddetinin iki ve üç boyutlu profilleri ayrıntılı olarak incelenmiştir. Alıcıdaki ışık şiddeti, farklı kaynak boyutlarında ve dalga boylarında incelenmiştir ve alıcıdaki ışık şiddetinin artan yayılma mesafesinde azaltıldığı gözlemlenmiştir. Bu çalışmada, alıcıdaki

pırıldama indeksi ve ışık şiddetinin hesaplanması için MATLAB kodları kullanılmıştır. Ayrıca, farklı türbülans değerlerinde, SLG ışık hüzmesi derecesi değiştirilerek, Gauss ışık hüzmesi için pırıldama indeksi değerleri elde edilerek, alınan sonuçların doğruluğu, Gauss ışık hüzmesi için literatürde daha önce alınan sonuçlar ile karşılaştırılarak test edilmiştir.

**Anahtar Kelimeler:** Alıcı açıklığı pırıldama indeksi, SLG, nokta-pırıldama indeksi, Rasgele Fazlı Ekran yöntemi.





## ACKNOWLEDGEMENTS

I am delighted to convey my sincere appreciation to Assistant Professor Dr. Serap Altay Arpali, Dr. Çağlar Arpali and Prof. Dr. Halil Tanyer Eyyuboğlu for their supervision, special guidance, suggestions, and encouragement throughout the development of this thesis.

I would like to thank Al-Nahrain University of the Ministry of Higher Education in Iraq for its financial support. None of my achievements would have been possible without their constant encouragement and support.

To my committee, Professor Halil Tanyer Eyyuboğlu and Assistant Professor Serap Altay Arpali and Assistant Professor Nursel Akçam, I give them thanks.

My sincere thanks go to my family for their patience, understanding and love. Nothing would have been possible without their constant encouragement and support.

I acknowledge and sincerely thank and offer my appreciation to my son (Assad Hussein Thary, M.Sc.) for his help and support.

Finally, I wholeheartedly express my grateful feelings to my friends in Iraq and Turkey.

## TABLE OF CONTENTS

STATEMENT OF NON -PLAGIARISM.....	iii
ABSTRACT.....	iv
ÖZ.....	vi
ACKNOWLEDGEMENTS.....	viii
TABLE OF CONTENTS.....	ix
LIST OF FIGURES.....	xi
LIST OF ABBREVIATIONS.....	xv
LIST OF SYMBOLS.....	xvi

### CHAPTERS:

<b>1.</b>	<b>INTRODUCTION.....</b>	<b>1</b>
	<b>1.1.</b> Preface.....	1
	<b>1.2.</b> Objectives.....	5
	<b>1.3.</b> Organization of the Thesis.....	5
<b>2.</b>	<b>LASER BEAM PROPAGATION.....</b>	<b>6</b>
	<b>2.1.</b> Paraxial Wave Equation.....	6
	<b>2.2.</b> Paraxial approximation .....	7
	<b>2.3.</b> Optical Wave Models .....	9
	<b>2.4.</b> Plane Wave and Spherical Wave Models .....	9

2.5.	Lowest-order Gaussian-beam Wave.....	11
2.6.	Solution of Paraxial Equation.....	13
	2.6.1 The Huygens Fresnel Integral.....	14
	2.6.2 The Rytov Approximation.....	14
2.7.	Atmospheric Effects on Laser beam Propagation.....	15
2.8.	Optical Turbulence .....	16
3.	THE PROPAGATION AND AVERAGE INTENSITY OF SLG BEAM.....	17
	3.1. Super Lorentz Gaussian beam .....	17
	3.2. Intensity in the Source Plane.....	19
	3.3. Average Intensity in the Receiver Plane.....	19
	3.4. Numerical Calculations and Results.....	20
4.	EVALUATION THE SCINTILLATION INDEX OF SLG BEAM BY NUMERICAL METHOD.....	30
	4.1. Random Phase Screen Method.....	30
	4.2. Aperture Averaged Scintillation of SLG beam and Numerical Results.	32
5.	CONCLUSION AND FUTURE SCOPE.....	42
	5.1. Conclusion.....	42
	5.2. Future Scope.....	43
	REFERENCES.....	44
	A. CURRICULUM VITAE.....	A <sub>1</sub>

## LIST OF FIGURES

### FIGURES

<b>Figure 1</b>	The optical propagation system .....	7
<b>Figure 2</b>	Geometry of the paraxial approaching .....	8
<b>Figure 3</b>	Schematic illustration of the propagation geometry for plane wave.....	10
<b>Figure 4</b>	Schematic illustration of the propagation geometry for spherical waves.....	11
<b>Figure 5</b>	Amplitude profile of a Gaussian beam.....	12
<b>Figure 6</b>	Particular cases of radius of curvature: a) convergent beam, b) collimated beam, and c) divergent beam.....	13
<b>Figure 7</b>	Average receiver intensity of SLG <sub>22</sub> beam in two dimensions for different propagation distances.....	21
<b>Figure 8</b>	Source plane intensity profile of SLG <sub>11</sub> beam in three dimensions with the source sizes $w_{lxx} = w_{lyy} = w_{gxx} = w_{gyy} = 1cm$ .....	21
<b>Figure 9</b>	Average receiver intensity of SLG <sub>11</sub> beam in three dimensions for different propagation distances.....	22
<b>Figure 10</b>	Average receiver intensity of SLG <sub>11</sub> beam in two dimensions for different propagation distances.....	22
<b>Figure 11</b>	Source plane intensity profile of SLG <sub>10</sub> beam in three dimensions with the source sizes $w_{lxx} = w_{lyy} = w_{gxx} = w_{gyy} = 1cm$ .....	23
<b>Figure 12</b>	Source plane intensity profile of SLG <sub>00</sub> beam in three dimensions with the source sizes $w_{lxx} = w_{lyy} = w_{gxx} = w_{gyy} = 1cm$ .....	23

<b>Figure 13</b>	Average receiver intensity of SLG <sub>10</sub> beam in two dimensions for different propagation distances.....	24
<b>Figure 14</b>	Source plane intensity profile of SLG <sub>00</sub> beam in three dimensions with the source sizes $w_{l_{sx}} = w_{l_{sy}} = w_{g_{sx}} = w_{g_{sy}} = 1cm$ .....	24
<b>Figure 15</b>	Average receiver intensity of SLG <sub>00</sub> beam in three dimensions for different propagation distances.....	25
<b>Figure 16</b>	Average receiver intensity of SLG <sub>00</sub> beam in two dimensions for different propagation distances.....	25
<b>Figure 17</b>	Contour plot of source field intensity of SLG <sub>11</sub> beam and source sizes $w_{l_{sx}} = w_{l_{sy}} = 1cm$ , $w_{g_{sx}} = w_{g_{sy}} = 3cm$ .....	26
<b>Figure 18</b>	Contour plot of source field intensity of SLG <sub>10</sub> beam and source sizes $w_{l_{sx}} = w_{l_{sy}} = 1cm$ , $w_{g_{sx}} = w_{g_{sy}} = 3cm$ .....	26
<b>Figure 19</b>	Contour plot of source field intensity of SLG <sub>01</sub> beam and source sizes $w_{l_{sx}} = w_{l_{sy}} = 1cm$ , $w_{g_{sx}} = w_{g_{sy}} = 3cm$ .....	27
<b>Figure 20</b>	Contour plot of source field intensity of SLG <sub>00</sub> beam and source sizes $w_{l_{sx}} = w_{l_{sy}} = 1cm$ , $w_{g_{sx}} = w_{g_{sy}} = 3cm$ .....	27
<b>Figure 21</b>	Contour plot of source field intensity of different SLG beam orders.....	28
<b>Figure 22</b>	Source field of SLG <sub>01</sub> beam and the source sizes $w_{l_{sx}} = w_{l_{sy}} = 1cm = w_{g_{sx}} = w_{g_{sy}} = 1cm$ .....	28
<b>Figure 23</b>	Numerical and analytical calculations of the source field of SLG <sub>01</sub> with the source sizes $w_{l_{sx}} = w_{l_{sy}} = w_{g_{sx}} = w_{g_{sy}} = 1cm$ .....	29
<b>Figure 24</b>	Modelling propagation in turbulence via random phase screen.	32

<b>Figure 25</b>	Comparison of point-like scintillation index curves from random phase screen setup for different wavelengths of an SLG <sub>22</sub> for $d_m = 10$ .....	34
<b>Figure 26</b>	Aperture averaged scintillation curves against propagation distance at a fixed aperture length with a different wavelength of an SLG <sub>22</sub> from random phase screen setup for $d_m = 100$ .....	35
<b>Figure 27</b>	Aperture averaged scintillation against propagation distance at fixed aperture length with different wavelength of an SLG <sub>11</sub> from random phase screen setup for $d_m = 100$ .....	35
<b>Figure 28</b>	Aperture averaged scintillation curves against propagation distance at fixed aperture length with different wavelength of an SLG <sub>00</sub> from random phase screen setup for $d_m = 100$ .....	36
<b>Figure 29</b>	Aperture averaged scintillation curves against propagation distance at fixed aperture length with different wavelength of an SLG <sub>10</sub> from random phase screen setup for $d_m = 100$ .....	36
<b>Figure 30</b>	Aperture averaged scintillation curves against propagation distance at fixed aperture length with a different source size of an SLG <sub>11</sub> from random phase screen setup, for $d_m = 100$ .....	37
<b>Figure 31</b>	Comparison of point-like scintillation index curves from random phase screen setup for different wavelength of an SLG <sub>10</sub> for $d_m = 10$ .....	37
<b>Figure 32</b>	Comparison of point-like scintillation index curves from random phase screen setup for different source size of SLG <sub>10</sub> for $d_m = 10, C_n^2 = 5 \times 10^{-16} m^{-2/3}$ .....	38

<b>Figure 33</b>	Comparison of point-like scintillation index curves from random phase screen setup for different wavelength of an SLG <sub>00</sub> , for $d_m = 10$ .....	38
<b>Figure 34</b>	Aperture averaged scintillation curves against propagation distance at fixed aperture length with different source size of an SLG <sub>11</sub> from random phase screen setup for $d_m = 100$ , $C_n^2 = 10^{-15} m^{-2/3}$ .....	39
<b>Figure 35</b>	Comparison of point-like scintillation index curves from random phase screen setup for different wavelength of an SLG <sub>11</sub> , for $d_m = 10$ .....	39
<b>Figure 36</b>	Aperture averaged scintillation curves against propagation distance at fixed aperture length with different source size of an SLG <sub>10</sub> from random phase screen setup for $d_m = 100$ , $C_n^2 = 5 \times 10^{-16} m^{-2/3}$ .....	40
<b>Figure 37</b>	Aperture averaged scintillation curves against propagation distance at fixed aperture length with different source size of an SLG <sub>10</sub> from random phase screen setup for $d_m = 100$ , $C_n^2 = 10^{-15} m^{-2/3}$ .....	40
<b>Figure 38</b>	Variation of scintillation curves against propagation distance at fixed aperture length with different $d_m$ (side length of square aperture) of an SLG <sub>10</sub> from random phase screen setup.....	41
<b>Figure 39</b>	Aperture averaged scintillation curves against propagation distance at fixed aperture length with different SLG beam order from random phase screen setup for $d_m = 100$ , $C_n^2 = 10^{-15} m^{-2/3}$ .....	41

## LIST OF ABBREVIATIONS

SLG	Super Lorentz Gaussian Beam
SLG <sub>00</sub>	Super Lorentz Gaussian Beam of Zero Beam Order
SLG <sub>11</sub>	Super Lorentz Gaussian Beam of First Beam Order
SLG <sub>22</sub>	Super Lorentz Gaussian Beam of Second Beam Order
TEM <sub>00</sub>	Transvers Electromagnetic Mode
RPS	Random Phase Screen Method
MIMO	Multi-Input Multi-Output
HD	High-Definition
RDO	Relative Diversity Order
BER	Bit Error Rate
UV	Ultra-Violate
RF	Radio Frequency



## LIST OF SYMBOLS

$U_0(s,0)$	The complex Field of Wave at Source Plane
$(f_x, f_y)$	Spatial Frequency in $x$ and $y$ Directions, Respectively
$k$	Wave Number
$\lambda$	Wavelength
$\delta(\mathbf{r})$	Dirac Delta
$\psi(r, s)$	Random Part of the Complex Phase by Rytov Method
$\psi_1(r, s)$	The First Order Perturbations
$\psi_2(r, s)$	The Second Order Perturbations
*	Conjugate Operator
$\langle \cdot \rangle$	Ensemble Average over the Random Medium
$\langle I(r, z) \rangle$	Average Intensity on Receiver Plane
$\langle I^2(r, z) \rangle$	Average of the Square Intensity on Receiver Plane
$L_r$	The side length of square aperture opening of the receiver Plane
$L_s$	Source Aperture Length
$C_n^2$	Structure Constant of Atmosphere in $m^{-2/3}$
$N_g$	Number of Grid Points
$N_R$	Number of Realization
$n\Delta z$	The total Distance Between Source and Receiver Planes
$A_0$	The Amplitude of Wave
$\phi(r_x, r_y)$	Spatial Phase Distribution
$d_1, d_2$	Grid Spacing on Source and Receiver Planes

$z$	Propagation Distance
$(w_{lx}, w_{ly})$	Super Lorentz Gaussian Source Sizes
$V(r, z)$	The Amplitude of the Receiver Field
$G(\mathbf{s}, \mathbf{r}; z)$	Green's Function
$m, n$	Beam order
$\mathbf{F}^{-1}$	Invers Fourier Transform Operator
$\mathbf{F}$	Fourier Transform Operator
$n$	Number of Interval Between two Screens
$\nabla$	Laplacian Operator
$(F_{gx}, F_{gy})$	Focal length Parameter
$U_{m,n}(s_x, s_y, z = 0)$	Source Field of SLG beam
$F_0$	Phase Front Radius of Curvature
$\phi_0$	Phase of the Wave
$r$	Radial Transverse Coordinate on Receiver Plane
$I_{m,n}(s_x, s_y, z = 0)$	Source Intensity of SLG beam
$U_0(r, 0)$	Gaussian Optical Field at Source Plane
$a_0$	The Amplitude of Gaussian Optical Field
$w_0$	Radius Spot Size
$m^2(z)$	Scintillation Index
$N_s$	Number of Phase Screens
$P(z)$	Power over a Limited Aperture Opening
$U_0(r, z)$	The Complex Amplitude of Wave at Receiver Field
$\Delta z$	Distance Between Two Screen Phases
$U_{m,n}^*(s_x, s_y, z = 0)$	Conjugate of Source Field of SLG beam
$U(r, z)$	The Receiver Field in Rytov Theory
$\alpha_0$	Complex parameter related to spot Size
$\mathbf{r}, \mathbf{s}$	Transverse Coordinate axes
$i$	Imaginary Number

$U^*(r, z)$	The Conjugate of Receiver Field
$U_s(s_x, s_y)$	The Source Field of the RPS Method
$U_r(r_x, r_y, z)$	The Receiver Field of the RPS Method
$h(r_x, r_y)$	The Spatial Response of the Propagating Medium
$d_m$	The Ratio Between the Side Length of the Square Aperture and the Grid Spacing at Receiver Plane



## CHAPTER I

### INTRODUCTION

#### 1.1 Preface

Intensity fluctuations occurring in a receiver plane are called scintillation in the optical beam and are produced by the turbulent nature of the atmosphere layers. These scintillations fade in a received signal. Consequently, there are several lessons to be learned in the work to decrease scintillation. The improvement of scintillation can be performed by using focused beams in an optical communication link [1]. Aperture averaging is one of the methods used to decrease the scintillation index. The effect of aperture averaging has been studied in the context of laser beam propagation in a turbulent atmosphere [2]. The plane wave of receiver aperture averaging effects have been studied in [2]. The turbulent atmosphere of the aperture length of a Gaussian beam is fixed. The average intensity is gained for a fixed beam into the receiver plane [3]. The propagation of Flat-Topped Gaussian beams can be performed when an accurate receiver that has a finite-sized aperture optical link is used in turbulent atmospheres [4]. In this study, the power scintillation and the receiver aperture averaging factor of collimated Super Lorentz Gaussian beams propagating in weak and moderate atmospheric turbulence are calculated. [4]. In spite of the lack of their communication range, free-space optics (FSO) refers to many potential compensations for radio frequency (RF) and fiber optical counterparts [5]. In addition to the comparison of the link of the RF system and FSO link donors, which have far higher data rates, there is no spectrum license and no frequency position being affected [6-7]. In the previous stages, optical wireless communications were changed. This is very important for development, normally identified as an FSO, due to the huge demand for a high data rate and data transmission for large level present applications, such as high-definition (HD)

content and the cloud, thereby adding to the amount of information to be transmitted. Hence, the bandwidth will vary in transmission. The applications in modern radio frequency (RF) technologies are applied in wireless services and are slower over a data stream network [8]. Furthermore, the satellite of optical communication systems is coming with extra advantages of the abovementioned wherever it is applied in FSO, and the fact that we observed the satellite-satellite links have reduced a turbulent atmosphere. However, the system capacity is a larger order of the optical beam divergence, at  $\mu$  rad wavelengths compared with an RF beam in the order of tens to hundreds of millirads [8]. FSO technology of wireless links is found wherever the sources of lasers are used. The optical wave spreads over a turbulent atmosphere, such as fog, rain, snow, haze, and normally for any free particle, which is affected due to a fading laser beam. Moreover, a turbulent atmosphere creates a propagated beam that increases the beam size [9]. The variations of optical communications through a turbulent atmosphere produces a faded signal [9]. The atmospheric turbulence as a sign of the temperature of the natural fluctuations in scintillation index appears [10]. The FSO system has a wide range of applications; some examples are last mile access, and innovative connectivity [9, 10]. There are also limits to FSO wavelengths which apply to military and civilian use [11]; deep space [12], inter-satellite [13], aerostat-to-ground [14], space-to-earth, ground-to-space [15] communication systems. In most cases, the atmosphere performs turbulence, which is described as three-dimensional air motions or currents in sizes ranging from millimeters to tens of meters. Turbulence in the atmosphere is the most effective transport mechanism and the refractive index of air is reduced by the degree of the humidity, such as heat and water vapor [16]. Atmospheric communication and imaging systems are limited to the turbulence in the atmosphere, that is, scintillations are decreased in the intensity of the received beam. Many academics have investigated the scintillation index and have worked on it both hypothetically and practically [17, 30]. Many books include the results of contributions in excellence [31, 32]. Intensity fluctuations of optical waves are exposed in these studies, as well as essential instructions of a turbulent atmosphere in the rules of both soft and strong turbulence. The Gaussian beam wave is the results of and fashioned from the limiting cases from these studies, which are clearly the spherical and cartesian coordinates of

plane waves. Collimated Annular beams approximately describe the scintillations for other types in [7], in addition to the types of beams being offered by Cowan et al [18]. Calculations of the scintillation index in the types of beams, such as Cos Gaussian beams and focused Annular beams, are not found in the literature. In these current studies, the new different beam types have been stated in the condition of a turbulent atmosphere, and overall beam types have been attained in the design. As different case solutions are obtained, as in [34], turbulence will protract the Flat-Topped Gaussian beam to deliver the intensity fluctuations and scintillation index of the beams. Solutions are randomly examined in [35]. The various types of source beam measure the performance of optic links, and the target of these actions are in free space. The kind of beam will vary the average intensity profile being received sideways on a turbulent path. Several scientists have studied the types of beams related to optical communications, such as the fundamental mode [36, 37], Laguerre Gaussian [38], higher order mode [39], Cosh Gaussian and Cos Gaussian [40, 41], Hermit Sine-Gaussian and Hermit Sinh Gaussian [42], Elliptical Gaussian [43], Lorentz beam [44], Flat-Topped [45], and the higher order Annular Gaussian [46]. These studies started making advanced developments later. The beams define fluctuation features by being numerically established, such as an optical vortex in the absence of turbulence, as in [7, 48]. When laser beams are propagated, they create weak atmospheric turbulence. The conditions of the analytical method and the Rytov method are investigated by means of the maximum frequency [7]. This is shown in [49-50], in which the vortex beams described the Rytov method depending on the direct application of mechanisms progressing to grave difficulties because the intensity turns out to be zero at the axis of the beam spreading in the constant medium. The Monte Carlo technique is applied in a numerical simulation, and the phase screens of beams make the laser beam propagate, as in [51]. Intensity fluctuations of vortex beams have calculated values. The mathematics do not allow us absolutely to judge the effect of the intensity fluctuation. The beam area cross section creates intensity fluctuations in [51]. The power spectral density function categorizes the scintillation index. The non-Kolmogorov properties are described in detail in the survey in [52-54]. Horizontal and slanting paths of atmospheric optical communication in the upper

layers of the atmosphere are measured as a non-Kolmogorov spectrum being formed by a direct method. The non-Kolmogorov nature of the spectrum is analyzed for its effect on distance propagation, which several studies have achieved. The link ranges are contacted in FSO systems, and the atmospheric turbulence is influenced depending on longer than 1-kilometer propagation distance; the received signal is decreasing [57]. More than a few authors have widely studied in [58, 62]. The wave fading mitigation technique has been newly studied [63, 64]. FSO communications are simulated in turbulence, particularly a weak description of the log-normal spreading of the beam. The relative diversity order (RDO) is accepted, which has been presented freshly in the background of the indoor RF log-normal channels. MIMO (multiple-input-multiple-output) helps in different FSO diversity schemes [65]. General application scenarios of the Flat-Topped Gaussian distribute unvarying intensity in the close field and the far field of remote sensing, tracing far expanse optical communication [66]. Various scientists have discussed the effects of turbulence on a Flat-Topped Gaussian beam. In ground-to-space optical communication, the Flat-Topped Gaussian beam that covers second-order path propagation properties has been studied; moreover, optical-wave oblique propagation in space has been studied [67-72]. Scintillation can lead to power losses at the receiver, resulting in a lower signal to noise ratio. For example, a Flat-Topped Gaussian beam can be used in an FSO link [73]. In slant path turbulence, the scintillation index of the Flat-Topped Gaussian beam is studied, including the intensity profile of atmospheric layers. The scintillation index of the Flat-Topped Gaussian beam in slant path turbulence is explored in theoretical simulations in [74-80]. There is also a study that considers in part a coherent Gaussian beam in atmospheric turbulence which is functional in FSO [78]. The scintillation is decreased because more fluctuations lead to power loss. Mainly in laser tracking and ranging systems [82, 83] and imaging systems [84, 85], Super Lorentz Gaussian beams have been studied along with the various features of small order beams. Super Lorentz Gaussian beams are being included in their vector range construction in far-field and out paraxial approaches [99-101]. The propagation into free space that can be treated in terms of the ABCD matrix [102, 103], the spreading of turbulence [104] and the beam propagation factors have been observed [105, 106]. The propagation

properties of Lorentz beam arrays have been similarly studied [107]. In this thesis we investigated power averaged scintillation index of SLG beam in the atmospheric turbulence which is not studied or investigated before.

## **1.2 Objectives**

The aim of this thesis is to explore the performance of the aperture averaged scintillation of SLG beam orders in a turbulent atmospheric system. For this purpose, we investigate and develop the effect of source sizes, wavelengths, beam orders, structure parameter and square aperture lengths through a variety of propagation distances on the power averaged scintillation in a moderately and weakly turbulent regime. Our objective is to design and analyze numerically the modelling of propagation in turbulence via a random phase screen method using MATLAB code models of the turbulent atmosphere.

## **1.3 Organization of the Dissertation**

This thesis consists of five chapters:

Chapter 1 – The introduction of this dissertation which holds the objective of the thesis.

Chapter 2 – The information in this chapter illustrates the laser beam propagation and some parameters of atmospheric turbulence is showed in details.

Chapter 3 – This chapter explains the receiver average intensity of SLG beam propagation through turbulence in an atmospheric layer.

Chapter 4 – This chapter presents the calculation of the scintillation index of SLG beam and simulation.

Chapter 5 – This chapter presents the conclusion and future work. It comprises the results of this dissertation, the results are applied in the optical communications, and performance is investigated in this study.



## CHAPTER II

### LASER BEAM PROPAGATION

#### 2.1 Paraxial Wave Equation

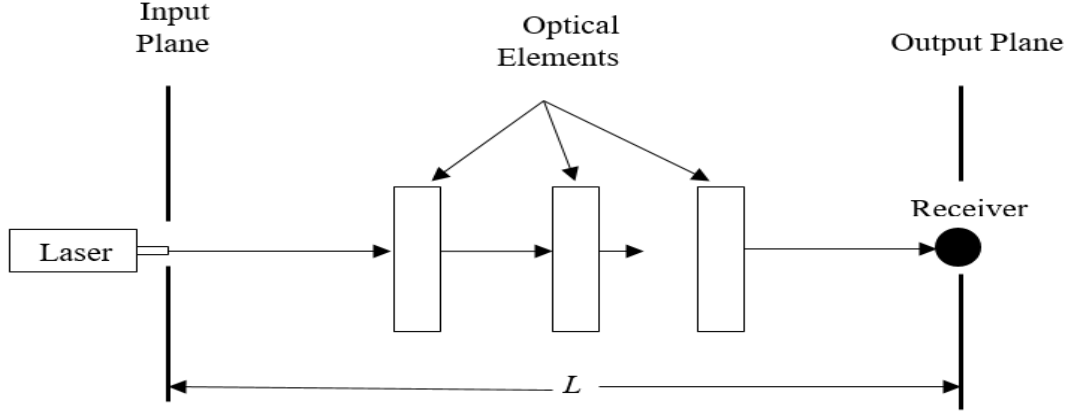
In general, when the optical wave is propagated through an atmosphere it suffers a fluctuation in amplitude and phase, leading to appearance of the scintillation effect. Figure 1 illustrates a general optical propagation system. The optical elements in Figure 1 cause the turbulence of the optical field at the output plane.

In the case of the electromagnetic radiation (laser beam) the governing equation of the field to describe the optical wave is called wave equation or Helmholtz equation and is given in [34] as

$$\nabla^2 U_0 + k^2 U_0 = 0, \quad (2.1)$$

Where  $\nabla^2$  is the laplacian operator,  $U_0$  is the complex amplitude of the wave, and  $k$  is the optical wave number related to the optical wavelength  $\lambda$  via  $k = \frac{2\pi}{\lambda}$ .

For optical wave propagation, we can further reduce the Helmholtz equation (2.1) to what is called the paraxial wave equation. To start, let us assume that the beam starts propagating in the plane at  $z = 0$  and broadcasts along the positive  $z$ -axis [34].



**Figure 1:** The optical propagation system [34]

The Helmholtz equation in cylindrical coordinates can be written as

$$\frac{1}{r} \frac{\partial}{\partial r} \left( r \frac{\partial U_0}{\partial r} \right) + \frac{\partial^2 U_0}{\partial z^2} + k^2 U_0 = 0 , \quad (2.2)$$

where  $r = \sqrt{(r_x^2 + r_y^2)}$  is the radial transverse coordinate.

For simplicity, we use  $U_0(r, z) = V(r, z)e^{ikz}$  to get the solution of paraxial wave equation. So, the paraxial approximation is given in [34], where  $U_0(r, z)$  is the complex amplitude of wave at the receiver plane,  $V(r, z)$  is the amplitude of the receiver field.

$$\frac{1}{r} \frac{\partial}{\partial r} \left( r \frac{\partial V}{\partial r} \right) + 2ik \frac{\partial V}{\partial z} = 0 , \quad (2.3)$$

## 2.2 Paraxial Approximation

In the paraxial approximation, it is assumed that the propagation distance for an optical wave along the z-axis is considerably bigger than the transverse spreading of the wave. Therefore,  $\mathbf{R} = (\mathbf{r}, z)$  and  $\mathbf{S} = (\mathbf{s}, 0)$  define two points in space where  $\mathbf{r}$  and  $\mathbf{s}$  are transverse coordinates of the axis of propagation, then the distance between these two points  $|\mathbf{R} - \mathbf{S}|$  is illustrated in Eq. (2.4) and Figure 2 [34]:

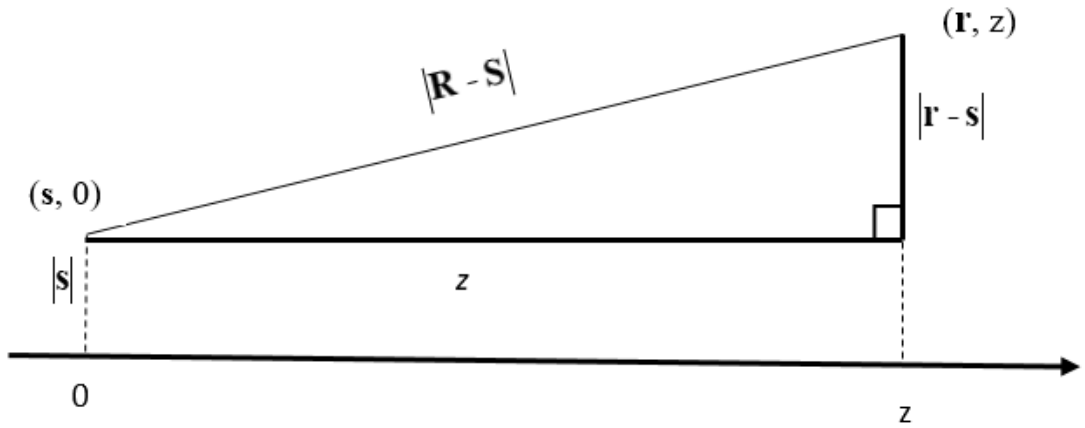
$$|\mathbf{R} - \mathbf{S}| = \sqrt{z^2 + (\mathbf{r} - \mathbf{s})^2} = z \left( 1 + \frac{(\mathbf{r} - \mathbf{s})^2}{z^2} \right), \quad (2.4)$$

where  $|\mathbf{r} - \mathbf{s}|$  is the distance between  $\mathbf{r}$  and  $\mathbf{s}$ .

The longitudinal distance is greater than the transverse distance between the dual points, then the second factor of Eq. (2.4) can be expanded in a binomial series to obtain the following [34].

$$|\mathbf{R} - \mathbf{S}| = z \left( 1 + \frac{(\mathbf{r} - \mathbf{s})^2}{2z^2} + \dots \right) = z + \frac{(\mathbf{r} - \mathbf{s})^2}{2z} + \dots, |\mathbf{r} - \mathbf{s}| \ll z, \quad (2.5)$$

Reducing all residual terms on the right-side of Eq. (2.5) behind the first two terms is called the paraxial approximation.



**Figure 2:** Geometry of the paraxial approximation [34]

### 2.3 Optical Wave Models

The optical wave propagation has focused on two models, namely, unbounded plane wave or spherical wave, the latter is often taken as a point source. But, the plane wave and spherical wave approximations are not enough to describe the propagation characteristics of the wave in several applications; especially when focusing and diverging features are important. In these cases, the lowest order of the Gaussian-beam wave model is usually considered, which lead to the plane and spherical wave models with limiting forms, also the higher-order Gaussian models in either rectangular or cylindrical coordinates are introduced for certain types of laser [34].

### 2.4 Plane Wave and Spherical Wave Models

A plane wave is described as one in which the equiphase surfaces (phase fronts) form parallel planes as shown in Figure 3. The mathematical formula of a plane wave in the source plane ( $z = 0$ ) is given in [34] by;

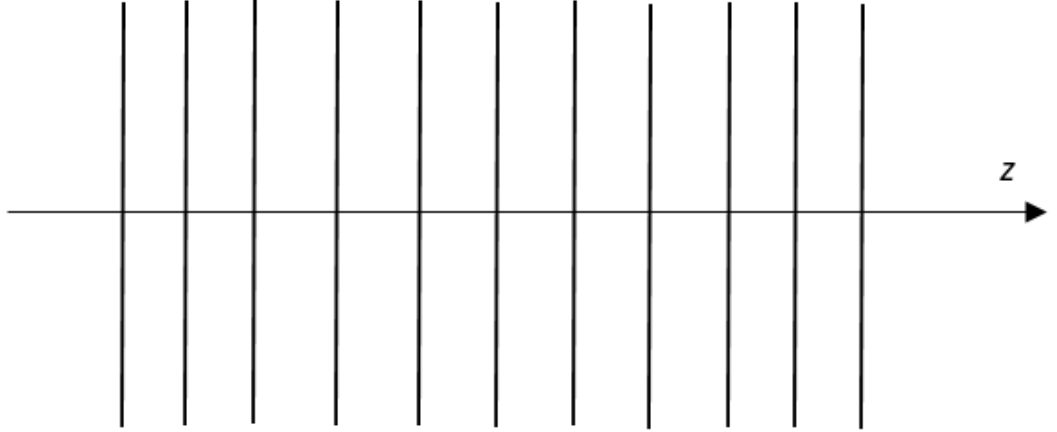
$$z = 0 \quad U_0(s,0) = A_0 e^{i\phi_0}, \quad (2.6)$$

where  $U_0(s,0)$  is the complex field of the wave at the source plane,  $A_0$  is the amplitude of the wave, and  $\phi_0$  is the phase of the wave.

If the plane wave is transferring along the positive  $z$ -axis in free space, the complex amplitude at distance propagation  $z$  from the source plane is given in [34] as;

$$z > 0 \quad U_0(r, z) = A_0 e^{i\phi_0 + ikz} = V(r, z) e^{ikz}, \quad (2.7)$$

where the  $V(r, z) = A_0 e^{i\phi_0}$  represents a solution of the paraxial wave equation.



**Figure 3:** Schematic illustration of the propagation geometry for plane waves [34]

Now the second model of wave is the spherical wave. In general, the spherical wave is generated by a spherical source as shown in Figure 4. In a homogeneous medium, the amplitude of the intensity remains constant, but the amplitude of the spherical wave is decreased while it is passing to the propagation distance. An original form of a spherical wave at source plane is given in [34] as:

$$z = 0 \quad U_0(s,0) = \lim_{R \rightarrow 0} \frac{A_0 e^{ikR}}{4\pi R} \cong A_0 \delta(\mathbf{r}) \quad . \quad (2.8)$$

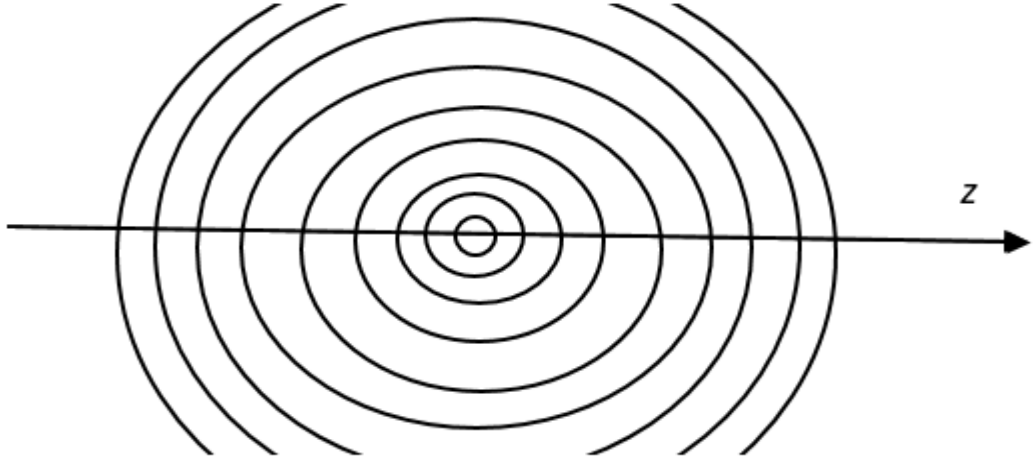
where  $\delta(\mathbf{r})$  is the Dirac delta function.

At a propagation distance  $z$  from the source plane, the spherical wave is described as

$$z > 0 \quad U_0(r, z) = \frac{A_0}{4\pi z} \exp\left[ikz + \frac{ikr^2}{2z}\right] = A \exp\left[ik\left(z + \frac{r^2}{2z}\right)\right] \quad , \quad (2.9)$$

where the magnitude  $A = A_0/4\pi z$  is scaled by propagation distance  $z$  and the phase

$\phi_0 = k\left(z + \frac{r^2}{2z}\right)$  has a transverse radial dependency.



**Figure 4:** Schematic illustration of the propagation geometry for spherical waves [34]

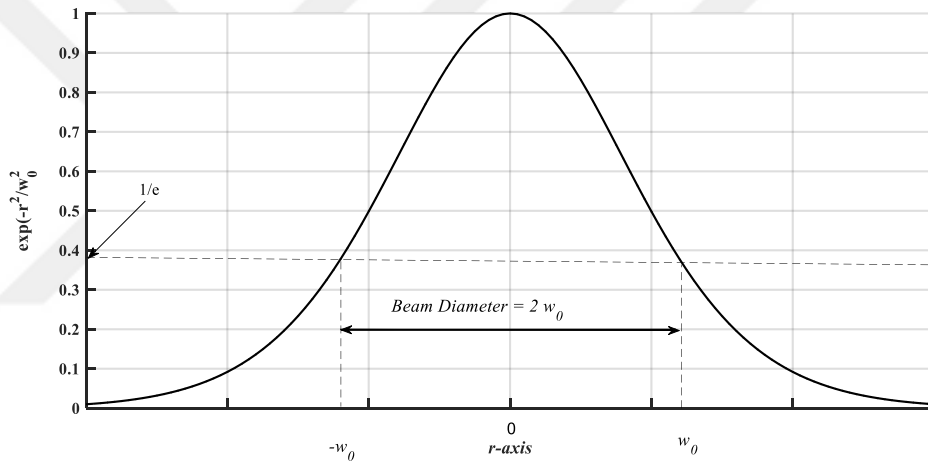
## 2.5 Lowest-order Gaussian-beam Wave

A lowest-order Gaussian-beam wave is called a  $TEM_{00}$ . At a propagation distance  $z = 0$ , the aperture is located and the distribution of amplitude is a Gaussian of radius  $w_0$  [m], where  $w_0$  is defined as the radius when the field amplitude drops to  $1/e$  of the beam axis as shown in Figure 5. In addition, the phase front is occupied to be parabolic with a radius of curvature  $F_0$  [m]. The exact cases of factors are illustrated as  $F_0 = \infty$ ,  $F_0 > 0$  and  $F_0 < 0$  conforming to collimated, convergent and divergent beam forms as shown in Figure 6,  $TEM_{00}$  is the Transvers Electromagnetic Mode. The Gaussian optical field at  $z = 0$  plane is described in [34] by:

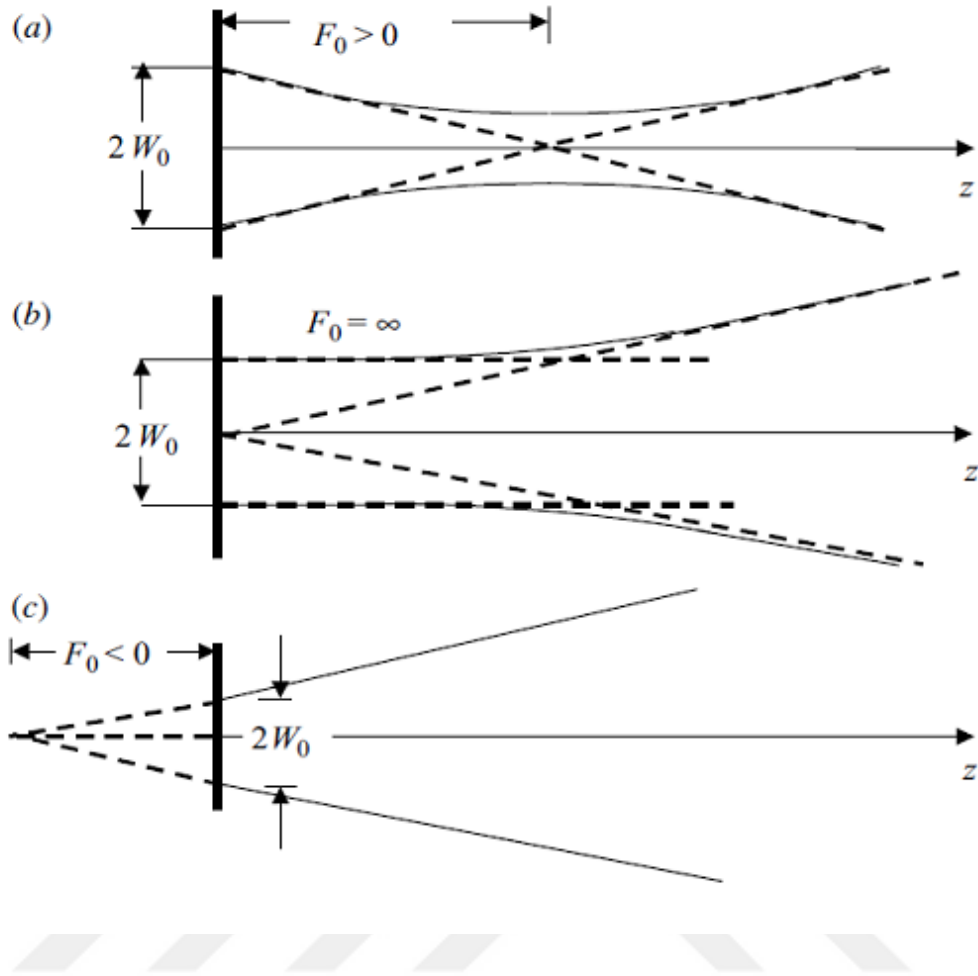
$$z = 0 \quad U_0(r,0) = a_0 \exp\left(-\frac{r^2}{w_0^2} - \frac{ikr^2}{2F_0}\right) = a_0 \exp(-0.5\alpha_0 kr^2), \quad (2.10)$$

where  $r = \sqrt{s_x^2 + s_y^2}$  is the radial coordinate on source plane from the beam center line,  $a_0$  is the amplitude of the Gaussian optical field,  $w_0$  is the beam radius (spot size), and  $\alpha_0$  is a complex parameter related to spot size and phase front radius of curvature according to

$$\alpha_0 = \frac{2}{kw_0^2} + i\frac{1}{F_0}. [m^{-1}] \quad (2.11)$$



**Figure 5:** Amplitude profile of a Gaussian beam [34]



**Figure 6** Particular cases of radius of curvature: a) convergent beam, b) collimated beam, and c) divergent beam [34]

## 2.6 Solution of Paraxial Equation

There are basically two methods of solution of paraxial equation which is described in Eq. (2.3). One method is called the Huygens Fresnel integral which applies when the optical element is inserted between input and output planes and the other method is the Rytov method which is used in the absence of optical elements between input (transmitter) and output (receiver) planes.



### 2.6.1 The Huygens Fresnel Integral

The Huygens-Fresnel integral provides another technique of analysis that leads to the results as Eqs. (2.7) and (2.9) for the complex amplitude at position  $z$  along the propagation path, but has the distinct advantage that it can be extended to the case where the propagation distance contains several optical elements arbitrarily distributed. The complex amplitude at propagation distance  $z$  from the source is represented by the Huygens-Fresnel integral in [34] as:

$$U_0(\mathbf{r}, z) = -2ik \int_{-\infty}^{\infty} \int G(\mathbf{s}, \mathbf{r}; z) U_0(\mathbf{s}, 0) d^2s, \quad (2.12)$$

where  $U_0(\mathbf{s}, 0)$  is the optical wave at the source plane,  $G(\mathbf{s}, \mathbf{r}; z)$  is the free-space Green's function,  $d$  is the derivation,  $k$  is a wave number.

In general, the free-space Green's function is a spherical wave which, under the paraxial approximation, is given in [34] by

$$G(\mathbf{s}, \mathbf{r}; z) = \frac{e^{ik|\mathbf{R}-\mathbf{S}|}}{4\pi|\mathbf{R}-\mathbf{S}|} \cong \frac{1}{4\pi z} \exp\left[ ikz + \frac{ik}{2z}|\mathbf{s}-\mathbf{r}|^2 \right]. \quad (2.13)$$

Where  $\mathbf{r}$  and  $\mathbf{s}$  are the transverse coordinates of the propagation axis and  $|\mathbf{R}-\mathbf{S}|$  is the distance between the two points which are located in the receiver and the source plane.

### 2.6.2 The Rytov Approximation

This approximation is used with the moderate-to-strong irradiance fluctuations. The optical field at propagation distance  $z$  from the source plane is represented in [34] by:

$$U(\mathbf{r}, z) = U_0(\mathbf{r}, z) \exp[\psi_1(\mathbf{r}, z) + \psi_2(\mathbf{r}, z) + \dots] . \quad (2.14)$$

where  $U_0(\mathbf{r}, z)$  is the unperturbed field,  $\psi_1(\mathbf{r}, z)$  and  $\psi_2(\mathbf{r}, z)$  represent first and second order perturbations, respectively,  $U(\mathbf{r}, z)$  is the receiver field in Rytov theory [34].

## 2.7 Atmospheric Effects of Laser Beam Propagation

There are many factors that have effect on the transmission of the optical wave through the atmosphere. These factors such as rain, snow, sleet, fog, haze, pollution, etc., that can critically limit the ability of the optical wave. The three primary atmospheric phenomena that disturb optical wave propagation are absorption, scattering, and refractive index fluctuations (i.e., optical turbulence). Absorption and scattering by the basic gases and particles of the atmosphere are wavelength dependent and give rise mainly to dropping of an optical wave. The index of refraction fluctuations leads to irradiance fluctuation, beam spreading, and loss of spatial coherence of the optical wave, among other effects. Diffraction and refraction of the wavefront by atmospheric inhomogeneities cause the most severe time varying effects. Air of randomly varying refractive index moving across the path produces fluctuations in phase velocity, thus distorting the wavefront. As the disturbed wavefront progresses, fluctuations develop in beam size, beam position, and intensity distribution within the beam. For a coherent beam, interference may occur between different portions of the wavefront. Unfortunately, these detrimental effects have far-reaching consequences on free-space optical communications, remote sensing, laser radar, and other applications that require the transmission of optical waves through the atmosphere [34].

## 2.8 Optical Turbulence

Optical turbulence is the fluctuation in the index of refraction, resulting from small temperature fluctuations. Random space-time redistribution of the refractive index causes a variety of effects on an optical wave related to its temporal irradiance fluctuations (scintillation) and phase fluctuations. The wavefront changes in the optical wave made by atmospheric turbulence result in a scattering of the beam (beyond that due to pure diffraction), random variations of the position of the beam centroid called beam wander, and a random reordering of the beam energy within a cross section of the beam important to irradiance fluctuations. In addition, the atmospheric turbulence that limits astronomical vision slowly destroys the spatial coherence of a laser beam as it propagates through the atmosphere [34]. Thus all details of the effect of optical turbulence on the Super Lorentz Gaussian (SLG) beam and intensity at the receiver plane using Random Phase Screen Method will be discussed in chapter four.

The propagation of Super Lorentz Gaussian (SLG) beam and the average intensity of it will be discussed in chapter three.

## CHAPTER III

### THE PROPAGATION AND AVERAGE INTENSITY OF THE SLG BEAM

In this chapter of the thesis we introduce the numerical calculations and results of the intensity of Super Lorentz Gaussian (SLG) beams at the source plane and the average intensity of SLG of wavelength  $\lambda = 1.55 \mu m$  after propagation distance  $z = 3.5 km$  with structure constant parameter  $C_n^2 = 10^{-15} m^{-2/3}$ .

#### 3.1 Super Lorentz Gaussian Beam

The formula of the source plane for Super Lorentz Gaussian (SLG) beams at  $z = 0$  is produced by multiplying Lorentz and Gaussian beams [110,111,112] :

$$U_{m,n}(s_x, s_y, z = 0) = \frac{s_x^m}{1 + s_x^2 w_{lsx}^{-2}} \frac{s_y^n}{1 + s_y^2 w_{lsy}^{-2}} \exp[-\pi \lambda^{-1} (w_{gx} s_x^2 + w_{gy} s_y^2)], \quad (3.1)$$

where  $U_{m,n}(s_x, s_y, z = 0)$  is the field of SLG beam at source plane, the factors  $(s_x, s_y)$  are the transverse coordinates of the source plane in  $x$  and  $y$  axes, respectively;  $(w_{lsx}, w_{lsy})$  are the Super Lorentzian Source Sizes,  $(m, n)$  are defined as the beam order,  $\lambda$  is the wavelength,  $z$  is the propagation distance and  $(w_{gx}, w_{gy})$  are given by

$$w_{gx} = 0.5\pi^{-1}\lambda w_{gsx}^{-2} + iF_{gx}^{-1}, \quad (3.2)$$

$$w_{gy} = 0.5\pi^{-1}\lambda w_{gsy}^{-2} + iF_{gy}^{-1}, \quad (3.3)$$

Where  $w_{gx}$  and  $w_{gy}$  are the Source Sizes of Gaussian beam, and  $(F_{gx}, F_{gy})$  indicate the focal length parameters in  $x, y$  axes, respectively [112, 113].

By applying Huygens-Fresnel Integral in free space to the source field in Eq. (3.4), the receiver field  $U(r, z)$  is given in [34] by:

$$U(r, z) = \frac{-ik}{2\pi z} \exp(ikz) \int \int_{-\infty}^{\infty} d^2s U(s, 0) \exp \left[ \frac{ik}{2z} |s - r|^2 \right] \exp[\psi(r, s)] , \quad (3.4)$$

Where  $U(s, 0)$  is optical field at source plane,  $\psi(r, s)$  is the random part of the complex phase by the Rytov method,  $r = (r_x, r_y)$  is the transverse coordinates which refer to the receiver plane,  $k$  is the optical wave number, the expression  $|s - r|^2$  is the distance between the transmitter and the receiver planes and is given by

$$|s - r|^2 = |s_x - r_x|^2 + |s_y - r_y|^2 , \quad (3.5)$$

$$|s - r|^2 = s_x^2 - 2r_x s_x + r_x^2 + s_y^2 - 2s_y r_y + r_y^2 , \quad (3.6)$$

For updating the Super Lorentz Gaussian beam using Extended Huygens-Fresnel integral by substituting Eq. (3.1) into Eq. (3.4), the output is given by a new expression as in Eq. (3.7):

$$U(r, z) = \frac{-ik}{2\pi z} \exp(ikz) \int \int_{-\infty}^{\infty} d^2s \frac{s_x^m}{1 + s_x^2 w_{lxx}^{-2}} \frac{s_y^n}{1 + s_y^2 w_{lyy}^{-2}} \exp \left[ -\pi \lambda^{-1} (w_{gx} s_x^2 + w_{gy} s_y^2) \right] \\ \times \exp \left[ \frac{ik}{2z} |s - r|^2 \right] \exp[\psi(r, s)] , \quad (3.7)$$

where  $s = (s_x, s_y)$  is the transverse coordinates that refer to the source plane [34].

### 3.2 Intensity in the Source Plane

The intensity distribution in the source plane of the Super Lorentz Gaussian (SLG) beam is characterized with the amplitude and phase. The intensity of the SLG beam at the source plane, denoted by  $I_{m,n}(s_x, s_y, z = 0)$ , is given by

$$I_{m,n}(s_x, s_y, z = 0) = U_{m,n}(s_x, s_y, z = 0)U_{m,n}^*(s_x, s_y, z = 0) , \quad (3.8)$$

where  $(s_x, s_y)$  are the transverse coordinates in the  $x$  and  $y$  axes, respectively, and  $*$  stands for conjugation, and  $U_{m,n}(s_x, s_y, z = 0)$  is the field of SLG beam at the source plane.

### 3.3 Average Intensity in the Receiver Plane

After appropriate propagation distance ( $z > 0$ ), the average intensity of the SLG beam is obtained by multiplying Eq. (3.5) with the conjugate of it. So the average intensity  $\langle I(r, z) \rangle$  at the receiver plane is illustrated as

$$\langle I(r, z) \rangle = \langle U(r, z)U^*(r, z) \rangle . \quad (3.9)$$

where  $\langle \cdot \rangle$  ensembles the average over the random medium statistics,  $U(r, z)$  is the receiver field of the SLG beam,  $U^*(r, z)$  is the conjugate of the receiver field of the SLG beam.

### 3.4 Numerical Calculations and Results

In this section, the numerical results are presented using Eqs. (3.1) and (3.9) as a function of the SLG beam. All numerical calculations and results are obtained by utilizing the random phase screen method which is developed by Halil Tanyer Eyyuboğlu [32]. The source and receiver fields, as well as the source and receiver intensities are defined in two and three dimensions leading to results that carry the same parameters. In the receiver plane, the average intensity profile of the Super Lorentz Gaussian beam is described in two and three dimensions. Several different source sizes and a specific wavelength of the receiver intensity are studied and calculated.

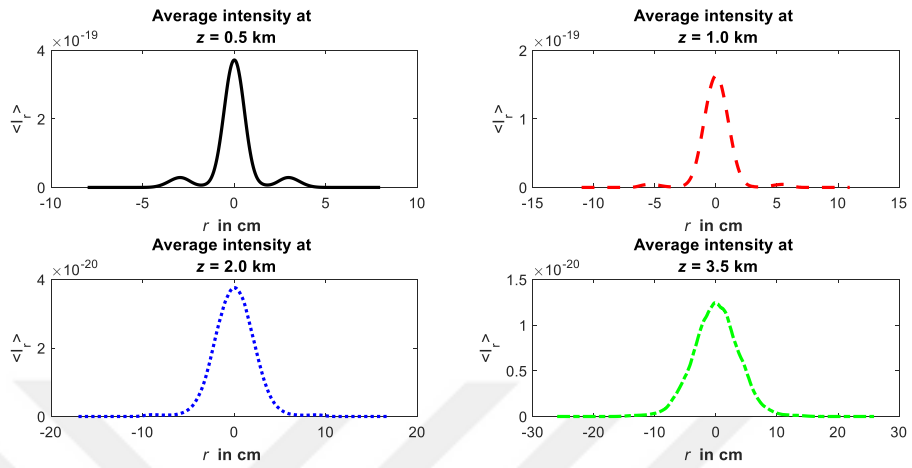
Figs. 7, 10, 13 and 16 display the average intensity of the SLG beam for different beam orders (SLG<sub>22</sub>, SLG<sub>11</sub>, SLG<sub>10</sub>, SLG<sub>00</sub>) in two dimensions with the source sizes ( $w_{lsx}$ ,  $w_{lsy}$ ,  $w_{gsx}$ ,  $w_{gsy}$ ) each equal to 1 cm,  $\lambda = 1.55 \mu m$ ,  $C_n^2 = 10^{-15} m^{-2/3}$ , the number of realization  $N_R = 500$  and  $F_{gx} = F_{gy} = \infty$ .

Figs. 8, 11 and 14 show the source intensity of the SLG beam in three dimensions with different beam orders (SLG<sub>11</sub>, SLG<sub>10</sub>, SLG<sub>00</sub>) at the same values of parameters which are used in two dimensions.

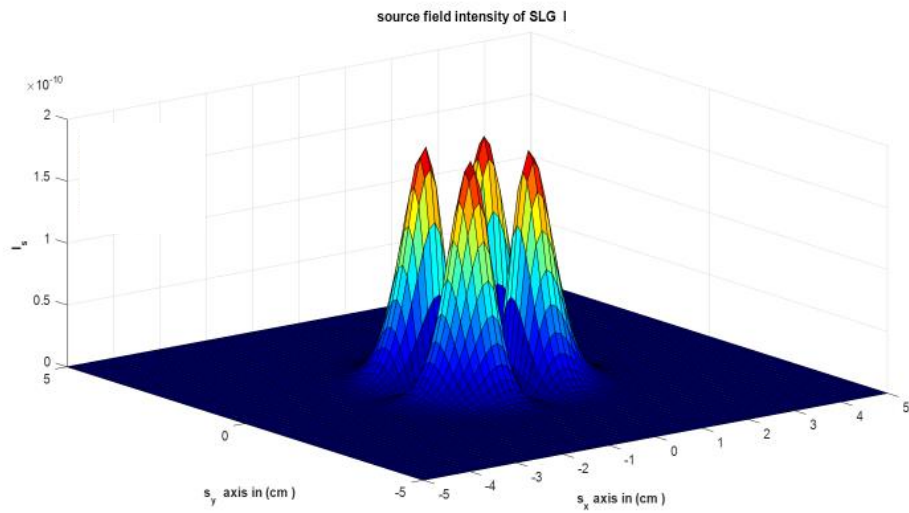
Figs. 9, 12 and 15 illustrate the receiver intensity of the SLG beam in three dimensions with different beam orders (SLG<sub>11</sub>, SLG<sub>10</sub>, SLG<sub>00</sub>).

Figs. 17, 18, 19 and 20 plot the contour of the source field intensity of the SLG beam with different beam orders (SLG<sub>11</sub>, SLG<sub>10</sub>, SLG<sub>01</sub>, SLG<sub>00</sub>) at wavelength  $\lambda = 0.8 \mu m$ . Figure 21 displays the contour of the source field intensity for all different beam orders of the SLG beam at the same values of source sizes.

Figs. 22 and 23 introduce the numerical and analytical results of the limiting cases for the field of the SLG<sub>01</sub> at the source plane in [116]. The value of the source sizes of the Gaussian beam is taken as  $w_{gsx} = w_{gsy} = 1 \text{ cm}$  and  $2 \text{ cm}$  numerically at a fixed propagation distance  $z$ . From our results, we observed that the magnitude of the average intensity is decreased and the form of it is expanded when the propagation distance is increased. Also we concluded that the Gaussian beam distribution is obtained when the beam order ( $m$ ,  $n$ ) of SLG is decreased.

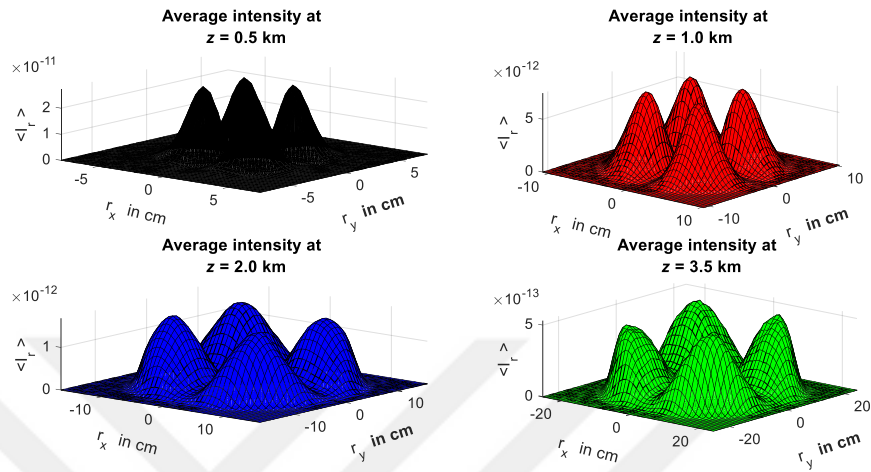


**Figure 7:** Average receiver intensity of SLG<sub>22</sub> beam in two dimensions for different propagation distances

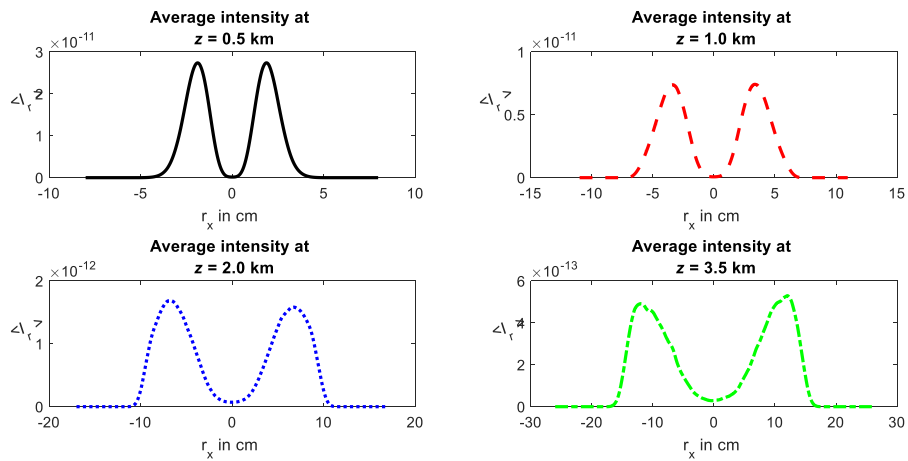


**Figure 8:** Source plane intensity profile of SLG<sub>11</sub> beam in three dimensions with the source sizes  $w_{lsx} = w_{lsy} = w_{gsx} = w_{g sy} = 1cm$

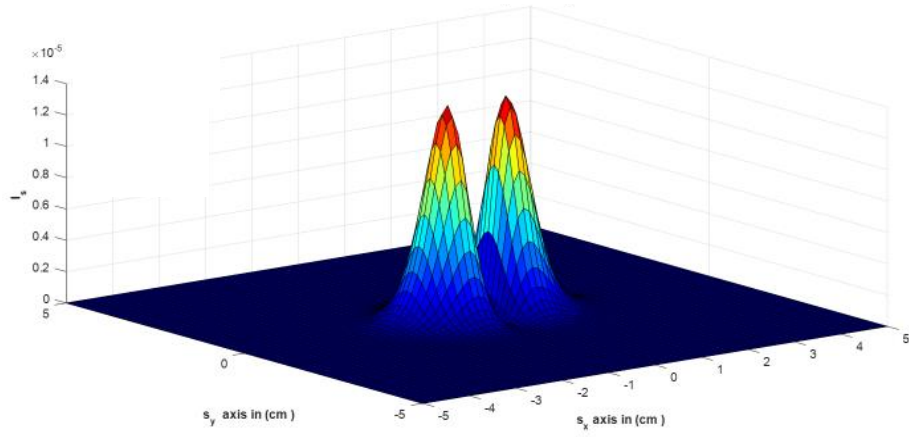




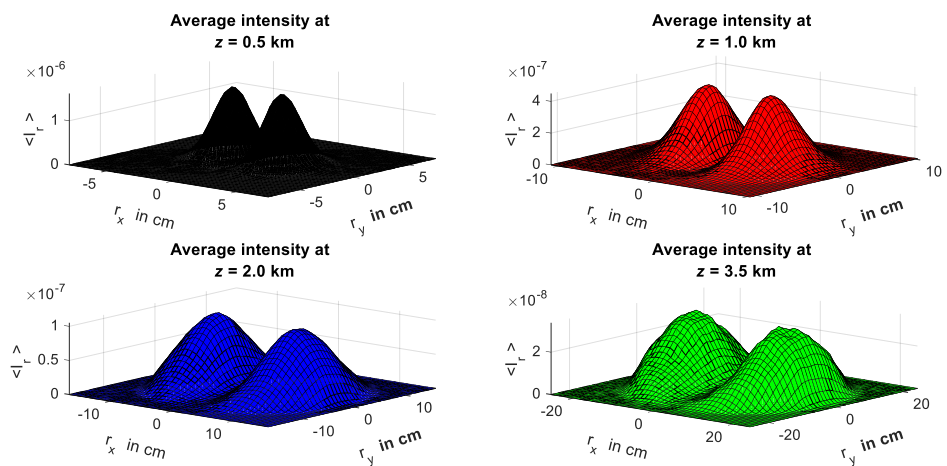
**Figure 9:** Average receiver intensity of SLG<sub>11</sub> beam in three dimensions for different propagation distances



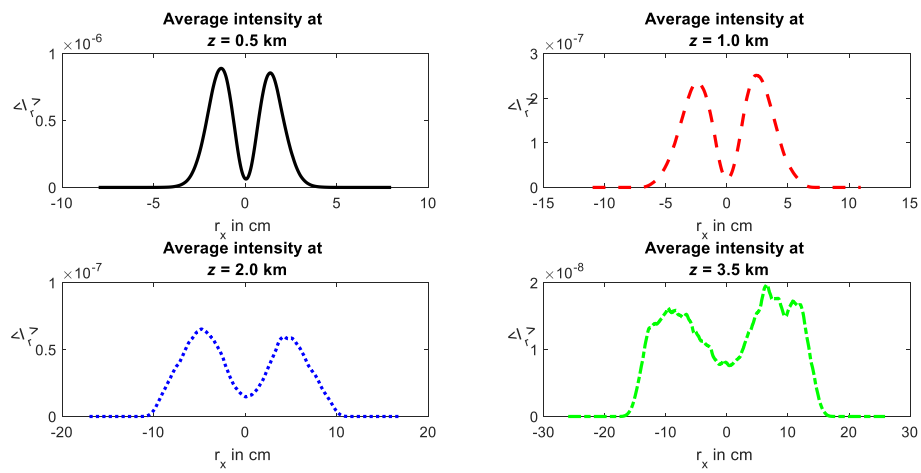
**Figure 10:** Average receiver intensity of SLG<sub>11</sub> beam in two dimensions for different propagation distances



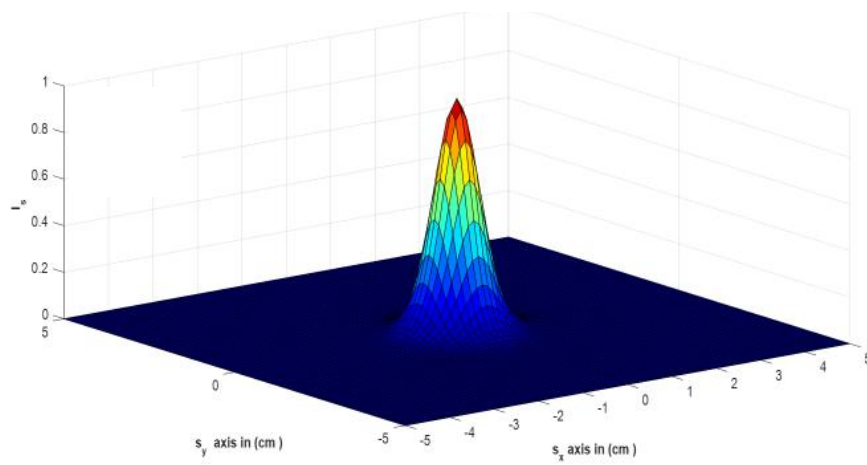
**Figure 11:** Source plane intensity profile of SLG<sub>10</sub> beam in three dimensions with the source sizes  $w_{lsx} = w_{lsy} = w_{gsx} = w_{gsy} = 1\text{cm}$



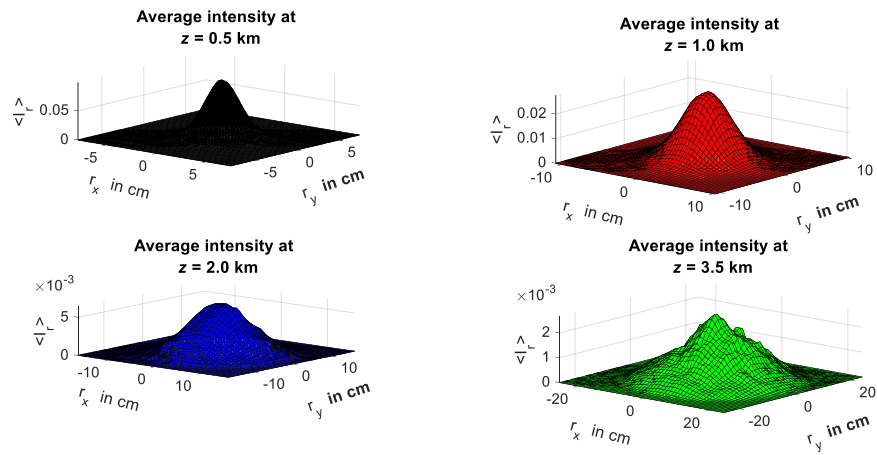
**Figure 12:** Average receiver intensity of SLG<sub>10</sub> beam in three dimensions for different propagation distances



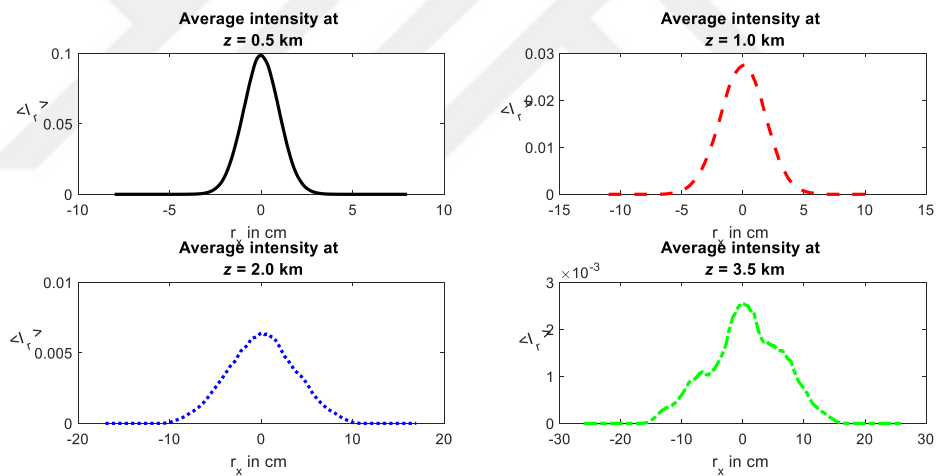
**Figure 13:** Average receiver intensity of SLG<sub>10</sub> beam in two dimensions for different propagation distances



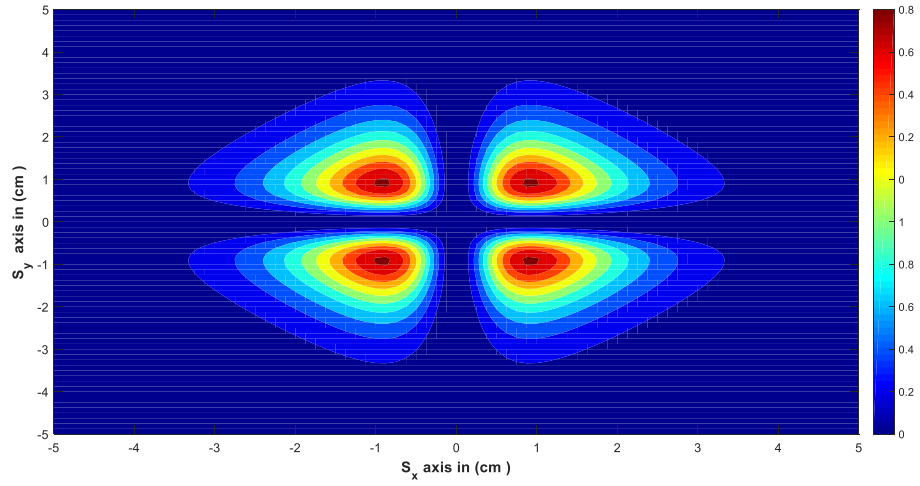
**Figure 14:** Source plane intensity profile of SLG<sub>00</sub> beam in three dimensions with the source sizes  $w_{lxx} = w_{lsy} = w_{gsx} = w_{gsy} = 1$  cm



**Figure 15:** Average receiver intensity of SLG<sub>00</sub> beam in three dimensions for different propagation distances

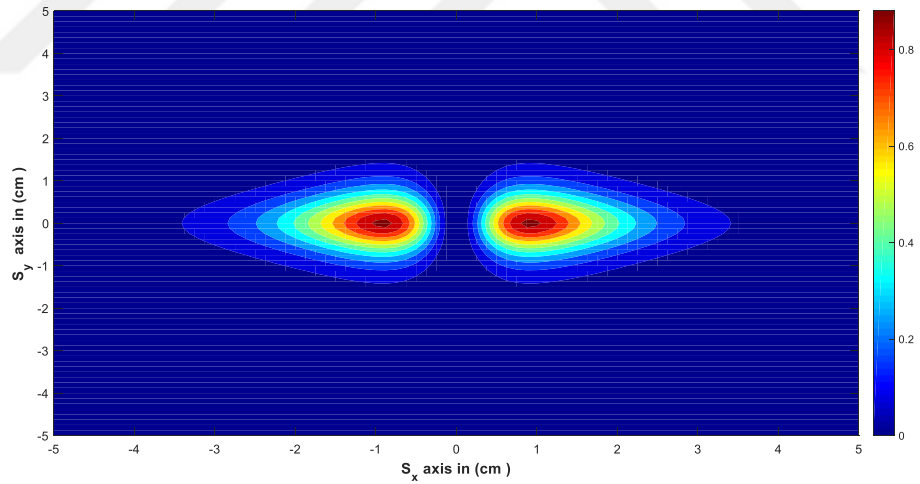


**Figure 16:** Average receiver intensity of SLG<sub>00</sub> beam in two dimensions for different propagation distances



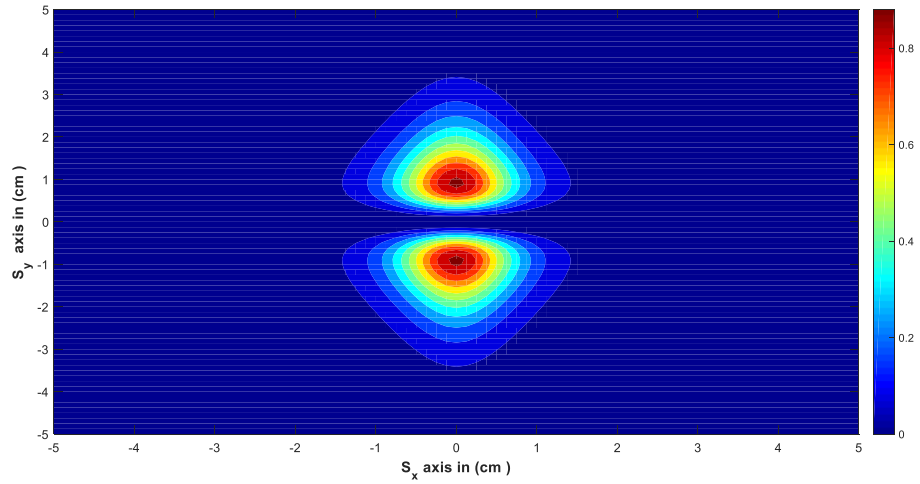
**Figure 17:** Contour plot of source field intensity of SLG<sub>11</sub> beam with source sizes

$$w_{lxx} = w_{lxy} = 1cm, \quad w_{gxx} = w_{gsy} = 3cm$$



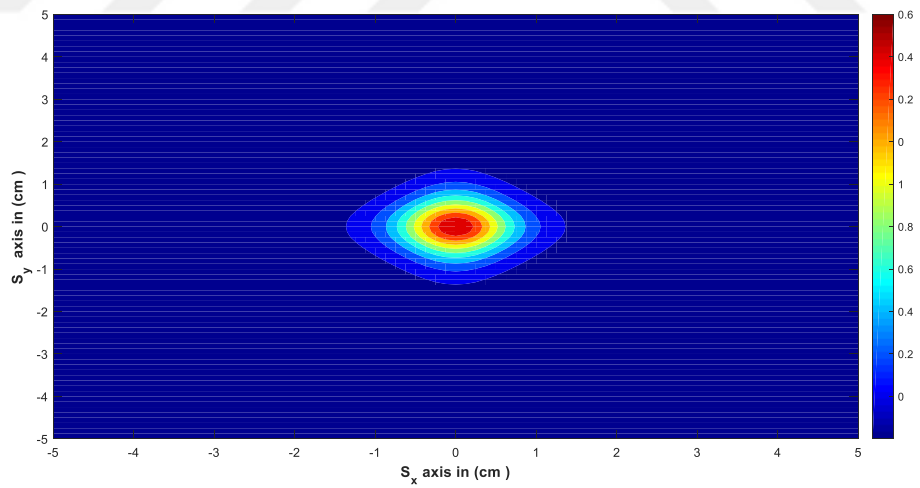
**Figure 18:** Contour plot of source field intensity of SLG<sub>10</sub> beam with source sizes

$$w_{lxx} = w_{lxy} = 1cm, \quad w_{gxx} = w_{gsy} = 3cm$$



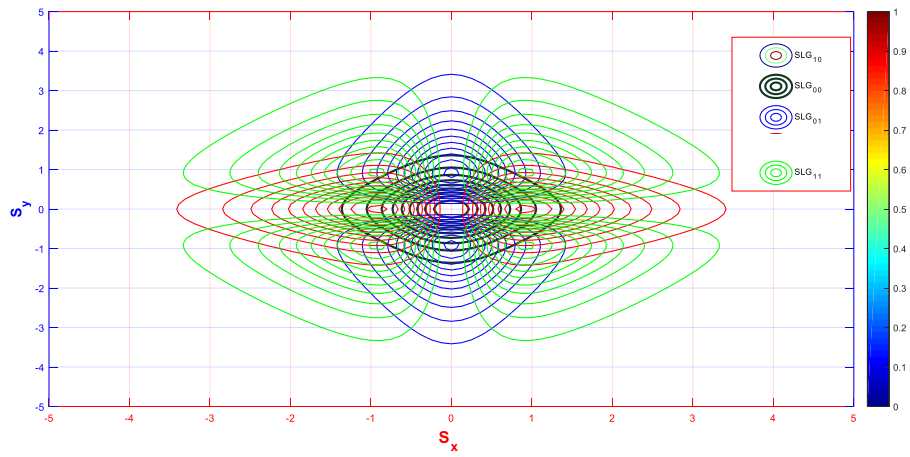
**Figure 19:** Contour plot of source field intensity of SLG<sub>01</sub> beam with source sizes

$$w_{l_{sx}} = w_{l_{sy}} = 1cm, \quad w_{g_{sx}} = w_{g_{sy}} = 3cm$$



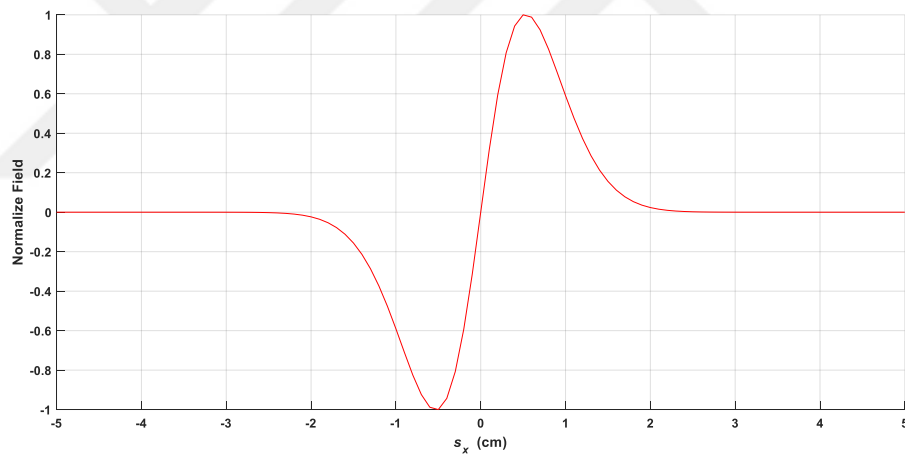
**Figure 20:** Contour plot of source field intensity of SLG<sub>00</sub> beam with source sizes

$$w_{l_{sx}} = w_{l_{sy}} = 1cm, \quad w_{g_{sx}} = w_{g_{sy}} = 3cm$$



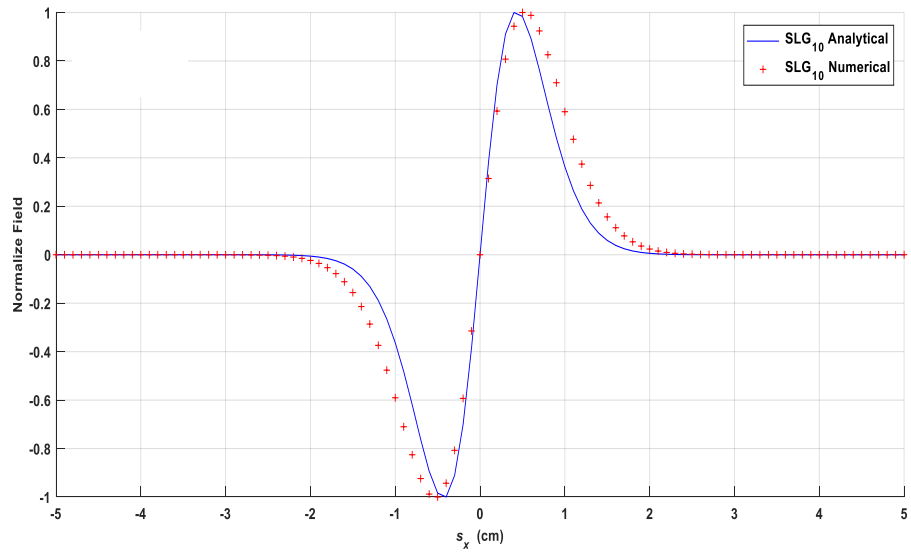
**Figure 21:** Contour plot of source field intensity of different SLG beam orders

$$w_{l_{sx}} = w_{l_{sy}} = 1\text{cm}, \quad w_{g_{sx}} = w_{g_{sy}} = 3\text{cm}$$



**Figure 22:** Source field of  $SLG_{01}$  beam with the source sizes

$$w_{l_{sx}} = w_{l_{sy}} = w_{g_{sx}} = w_{g_{sy}} = 1\text{cm}$$



**Figure 23:** Numerical and analytical calculations of the source field of SLG<sub>01</sub> with the source sizes  $w_{lxx} = w_{lxy} = w_{gxx} = w_{gxy} = 1cm$



## CHAPTER IV

### EVALUATION OF THE SCINTILLATION INDEX FOR SLG BEAM BY USING NUMERICAL METHOD

Many parameters have an effect on the atmospheric layer such as temperature, pressure, dust, humidity; that cause to diverge the optical beam which is propagated through these layers. Thus, the scintillation index is occurred due to variation in intensity and phase in atmospheric layer. In this chapter, the power scintillation of Super Lorentz Gaussian beams is investigated. The behavior of the SLG beam in moderately turbulent and weakly turbulent atmospheres is analyzed numerically using the random phase screen method.

#### 4.1 Random Phase Screen Model

Random Phase Screen (RPS) method has represented the propagation of SLG beam in turbulence medium and it is introduced by two new steps:

- a- A total of some random phase screens ( $N_s$ ) is placed between the source and receiver planes, in order to model the atmospheric turbulence as illustrated in Figure 24, and the modelling propagation in turbulence is evaluated by the method known as the random phase screen.

b- A number of realization denoted by  $(NR)$ , is used to run calculation in MATLAB code for approaching to the average numeric result. The mathematical model is illustrated in Eq. (4.1).

$$U_r(r_x, r_y, z) = \mathbf{F}^{-1} \left\{ \mathbf{F} [U_s(s_x, s_y)] \mathbf{F} [h(r_x, r_y)] \right\} = \mathbf{F}^{-1} [U_s(f_x, f_y) H(f_x, f_y)], \quad (4.1)$$

where  $U_r(r_x, r_y, z)$  is the receiver field of the RPS Method,  $U_s(s_x, s_y)$  is the source field of the RPS Method, the parameters  $(s_x, s_y)$  are the transverse coordinates in the source plane,  $h(r_x, r_y)$  is the spatial response of the propagating medium, the parameters  $(r_x, r_y)$  are the transverse coordinates in the receiver plane,  $\mathbf{F}$  signifies the Fourier Transform,  $\mathbf{F}^{-1}$  indicates the inverse operator, the parameters  $(f_x, f_y)$  describe the spatial frequency, the parameters  $H(f_x, f_y)$  and  $U_s(f_x, f_y)$  have the containment that the source and receiver planes are at the same scale or same increments.

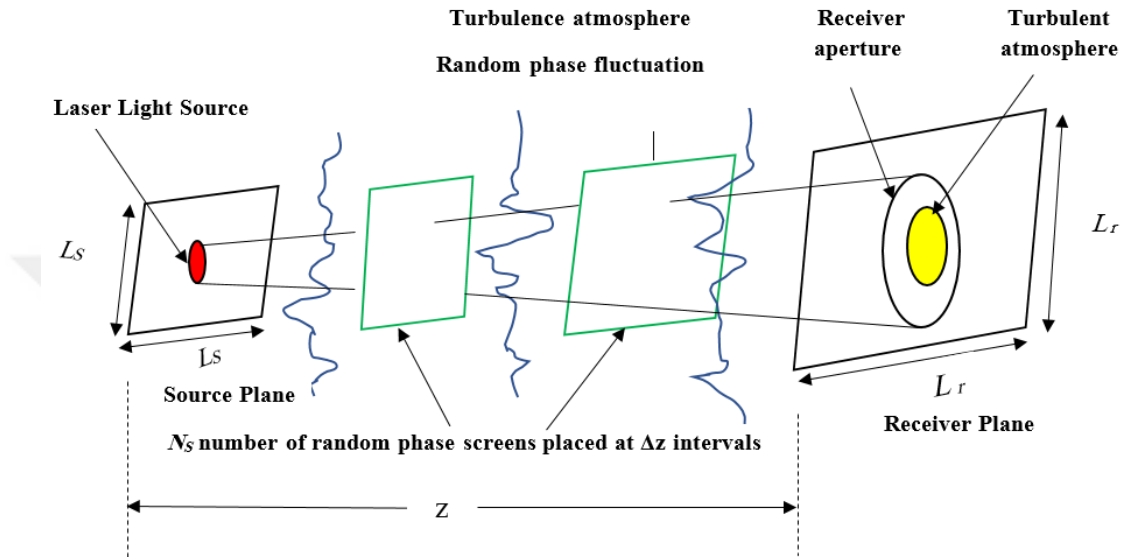
Thus, the behavior of the beam from  $(n-1)$  th to the  $n$ th screen is described in [32],  $U_r(r_x, r_y, n\Delta z)$  point towards the receiver field as shown:

$$U_r(r_x, r_y, n\Delta z) = \mathbf{F}^{-1} \left( \mathbf{F} \left\{ U_r[r_x, r_y, (n-1)\Delta z] \exp[j\phi(r_x, r_y)] \right\} H(f_x, f_y) \right), \quad (4.2)$$

$$P(z) = \int_{-0.5L_r}^{0.5L_r} \int_{-0.5L_r}^{0.5L_r} dr_x dr_y I(r_x, r_y, z) \quad , \quad m^2(z) = \frac{\langle P^2(z) \rangle}{\langle P(z) \rangle^2} - 1 \quad , \quad (4.3)$$

where  $L_r$  is the side length of square aperture opening of the receiver,  $\phi(r_x, r_y)$  denotes the spatial phase distribution derived from the power spectral density function,  $m^2(z)$  is the scintillation index,  $P(z)$  is the power over a limited aperture opening, the factor  $I(r_x, r_y, z)$  is the intensity on the receiver plane by Cartesian coordinates of the factors  $(r_x, r_y)$  is given in Eq. (3.11), the parameter  $n\Delta z$  refers to the total distance between two screens, and  $\Delta z$  is the distance between two screens.

Lastly, the aperture function had been transformed into minor and higher limits of gathering by spreading the square aperture slot into grids. Afterwards the fundamental of Eq. (4.3) had been calculated by substituting the second integral. The effect of fluctuation of the intensity is known as the irradiance covariance function [32].



**Figure 24:** Modelling propagation in turbulence via random phase screen method [32]

#### 4.2 Aperture Averaged Scintillation of SLG Beam and Numerical Results

In the receiver plane, the intensity fluctuation of SLG beam is occurred and it is called the scintillation. The scintillation is effected when some parameters are changed; such as the wavelengths, source sizes, beam order, and the side length of square aperture ( $L_r$ ). The conversion between the point-like scintillation and the aperture averaged scintillation depends on the side length of square aperture ( $L_r$ ). The grid spacing at the source and receiver planes,  $d_1$  and  $d_2$ , are determined in [32] by:

$$d_1 = \frac{L_s}{N_g}, \quad d_2 = 2.3438 \times 10^{-7} \times z + 1.9531 \times 10^{-4}, \quad (4.4)$$

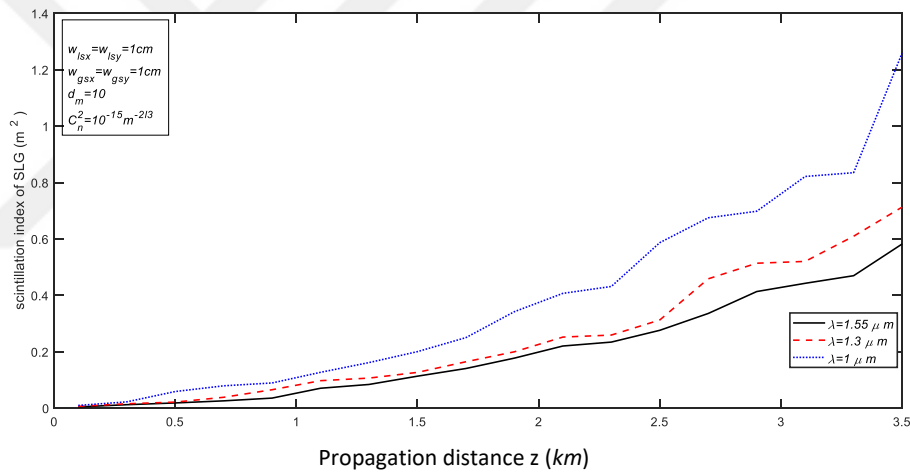
Depends on the grid spacing in the receiver plane  $d_2$ , the parameter  $d_m$  is the ratio between the side length of square aperture  $L_r$  and grid spacing  $d_2$  and it is determined in [32] by:

$$d_m = \frac{L_r}{d_2}, \quad (4.5)$$

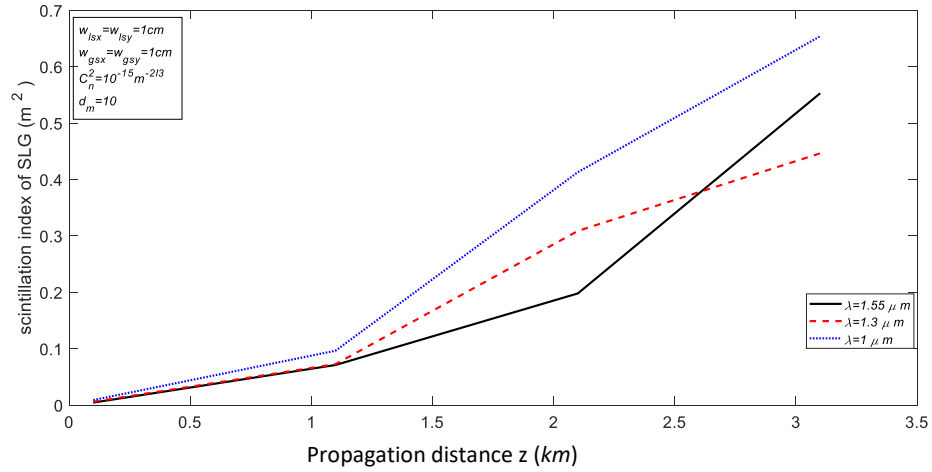
In our results, the value of Eq. (4.5) is considered as 10 and 100,  $L_s = 10$  cm, source sizes  $w_{gxx} = w_{gyy} = 1$  cm which refer to the Gaussian beam and source sizes  $w_{lsx} = w_{lsy} = 1$  cm which refer to the Lorentz beam, the wavelength ( $\lambda = 1.55 \mu\text{m}$ ), the number of realization ( $N_R = 500$ ), the focal length parameters ( $F_{gx} = F_{gy} = \infty$ ), the number of screen phase ( $N_S = 21$ ), the number of grid points ( $N_g = 512$ ). Based on these considered parameters, the power scintillation index of SLG beam orders with comparing between different wavelengths at  $d_m = 100$  [32].

Results of the aperture averaged scintillation at different  $d_m$  are shown in Figs 25, 26, 27, 28 and 29. These figures show the receiver aperture averaging is more useful for the SLG beam depending on the value of  $d_m$  and the power scintillation is decreased for SLG<sub>22</sub>, when compared to SLG<sub>00</sub>. Figs 25, 26, 27, 28 and 29 are described with the scintillation index against the propagation distance and they display different wavelengths  $\lambda$  with different SLG beam orders (SLG<sub>22</sub>, SLG<sub>11</sub>, SLG<sub>10</sub>, SLG<sub>00</sub>) and with fixed parameters such as focal length  $F_{gx}$ ,  $F_{gy}$ ; number of realization  $N_R$ , and the side length of square aperture  $d_m$ , and same source sizes ( $w_{lsx}$ ,  $w_{lsy}$ ,  $w_{gxx}$ ,  $w_{gyy}$ ). Figs 30, 31, 32, 33, 34, 35, 36 and 37, display the aperture averaged scintillation index and the point-like scintillation index for different source sizes from random phase screen setup. From Figs 30, 31, 32, 33, 34, 35, 36 and 37, we observed that a smaller scintillation index is obtained with large source size and small wavelength and also when compared to the point-like and power scintillations, we concluded that

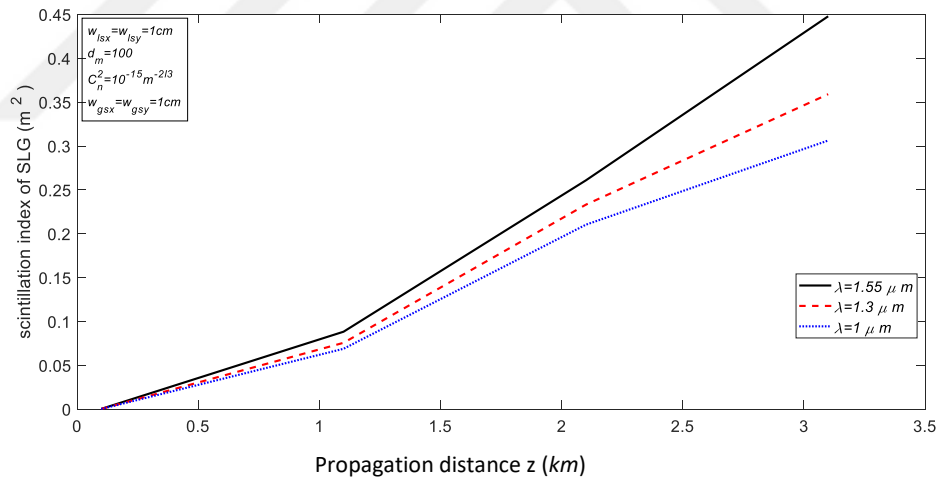
the least scintillation index appears with aperture averaged scintillation at  $d_m = 100$ . Figure 38 shows the  $SLG_{10}$  as a function of  $d_m$  with an enhancement of the structure parameter and we noticed that the scintillation index is decreased when  $d_m$  is increased and the least scintillation is obtained at  $d_m = 100$ . Figure 39 displays the numerical result of the power scintillation for different SLG beam orders with a fixed structure parameter  $C_n^2(m^{-2/3})$  and it illustrates that the  $SLG_{00}$  beam has the minimal scintillation. Finally, this work is an accepted paper in [118].



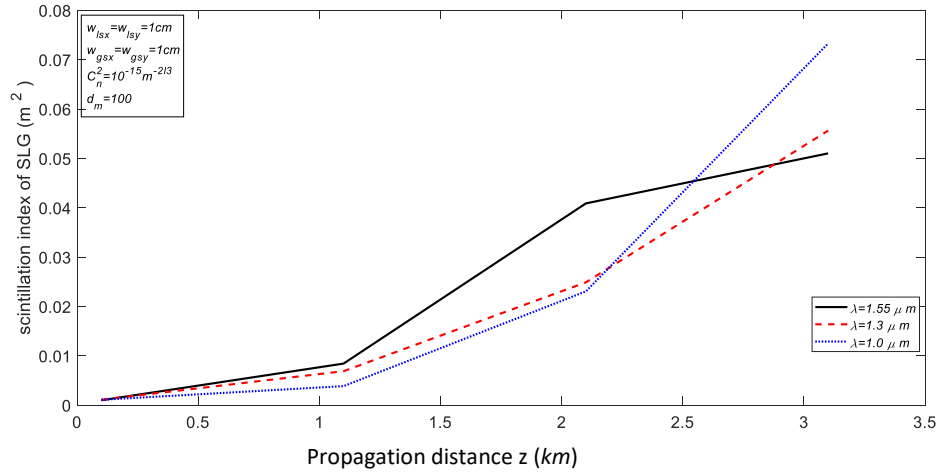
**Figure 25:** Comparison of point-like scintillation index curves from random phase screen setup for different wavelengths of an  $SLG_{22}$  for  $d_m = 10$



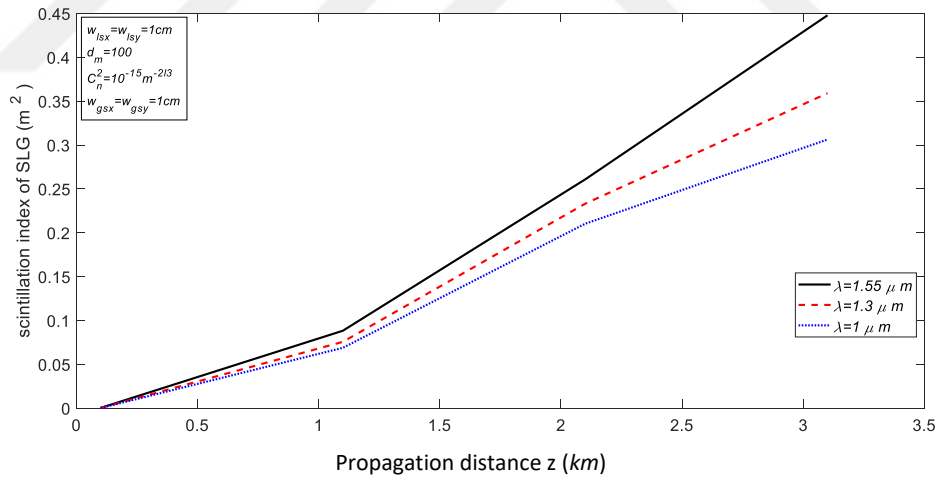
**Figure 26:** Aperture averaged scintillation curves against propagation distance at a fixed aperture length with a different wavelength of an  $SLG_{22}$  from random phase screen setup for  $d_m = 100$



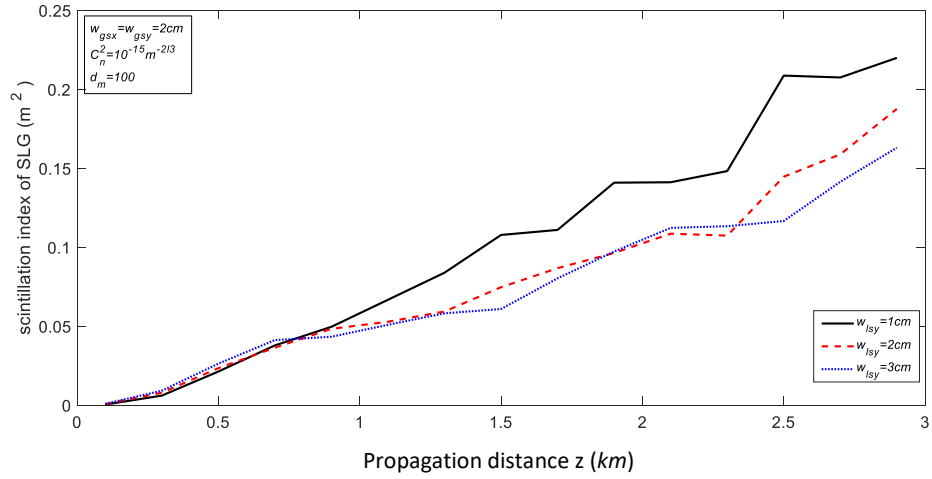
**Figure 27:** Aperture averaged scintillation against propagation distance at a fixed aperture length with different wavelength of an  $SLG_{11}$  from random phase screen setup for  $d_m = 100$



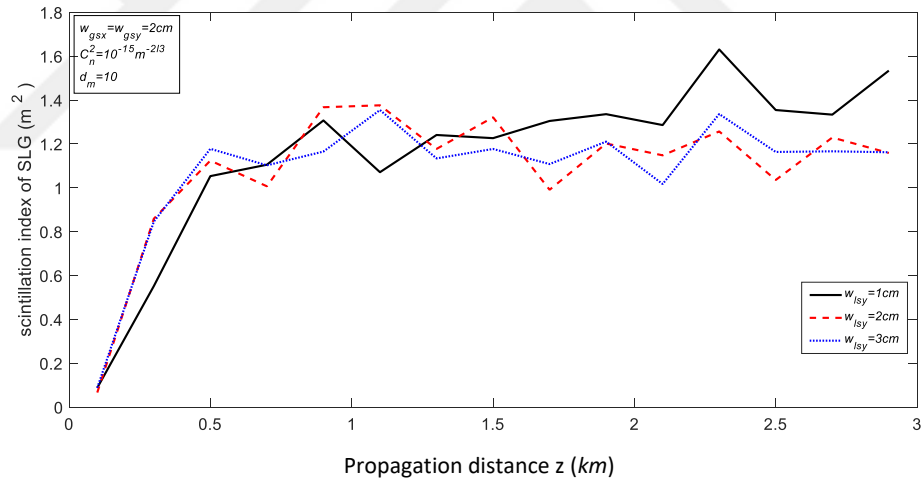
**Figure 28:** Aperture averaged scintillation curves against propagation distance at fixed aperture length with different wavelength of an  $SLG_{00}$  from random phase screen setup for  $d_m = 100$



**Figure 29:** Aperture averaged scintillation curves against propagation distance at fixed aperture length with different wavelength of an  $SLG_{10}$  from random phase screen setup for  $d_m = 100$

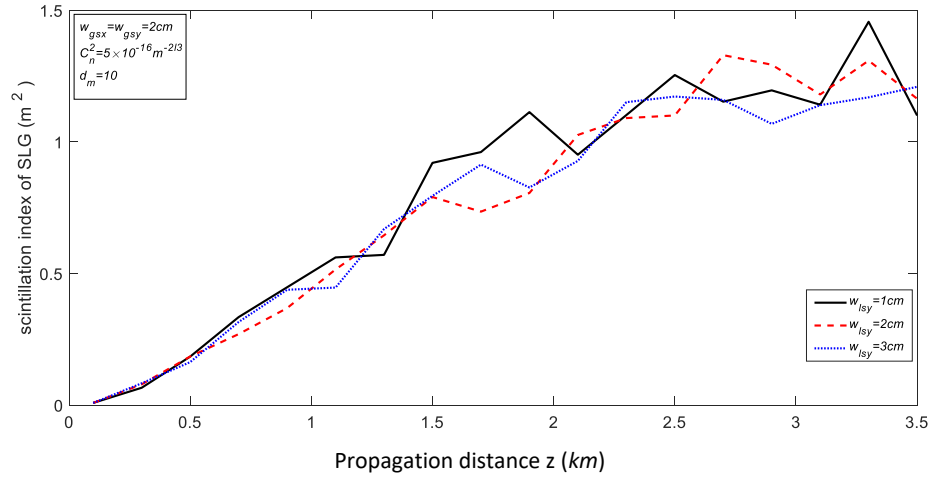


**Figure 30:** Aperture averaged scintillation curves against propagation distance at fixed aperture length with a different source size of an  $SLG_{11}$  from random phase screen setup for  $d_m = 100$

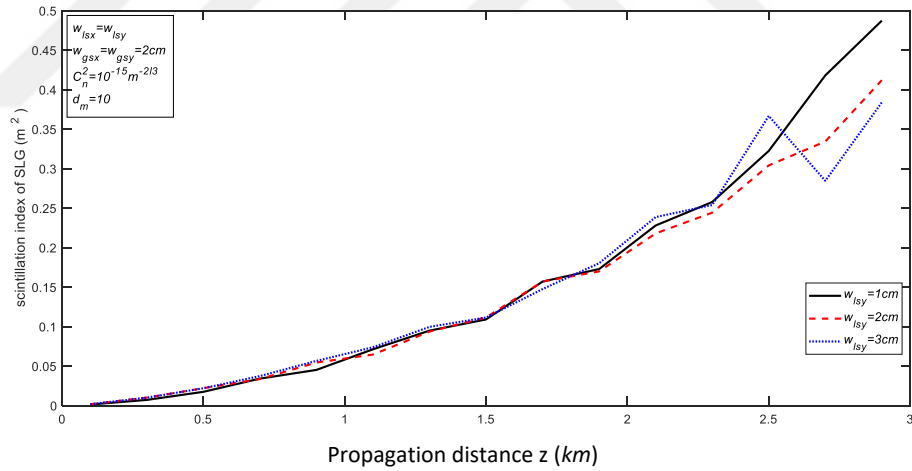


**Figure 31:** Comparison of point-like scintillation index curves from random phase screen setup for different wavelength of an  $SLG_{10}$  for  $d_m = 10$

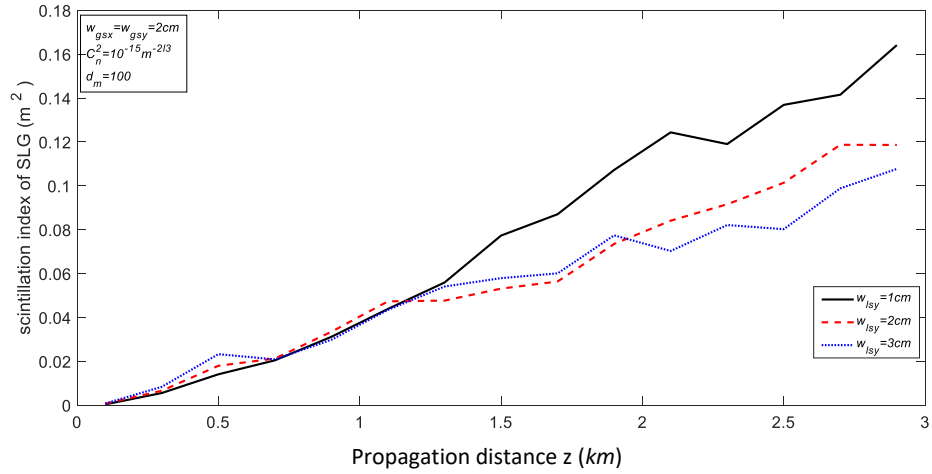




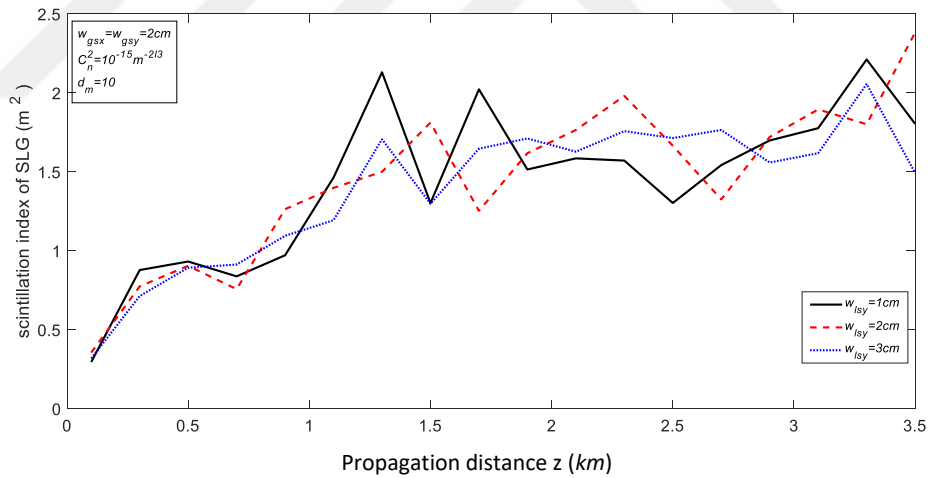
**Figure 32:** Comparison of point-like scintillation index curves from random phase screen setup for different source size of  $SLG_{10}$  for  $d_m = 10$ ,  $C_n^2 = 5 \times 10^{-16} m^{-2/3}$



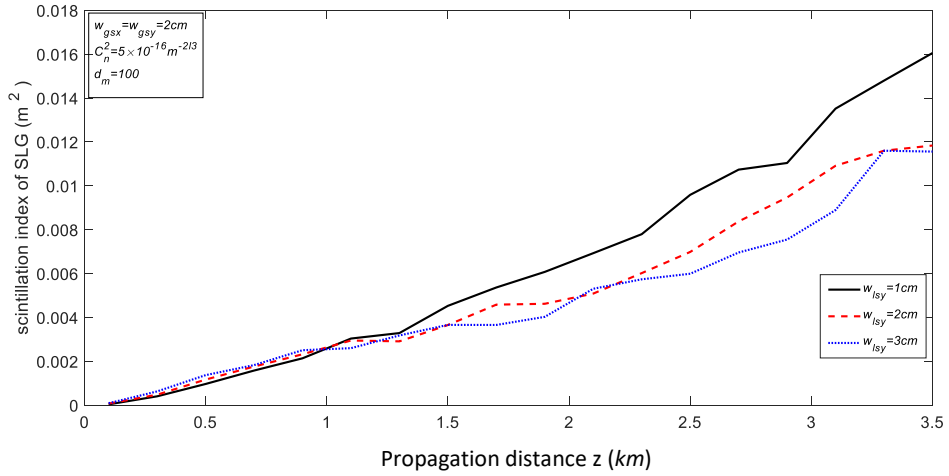
**Figure 33:** Comparison of point-like scintillation index curves from random phase screen setup for different wavelength of an  $SLG_{00}$  for  $d_m = 10$



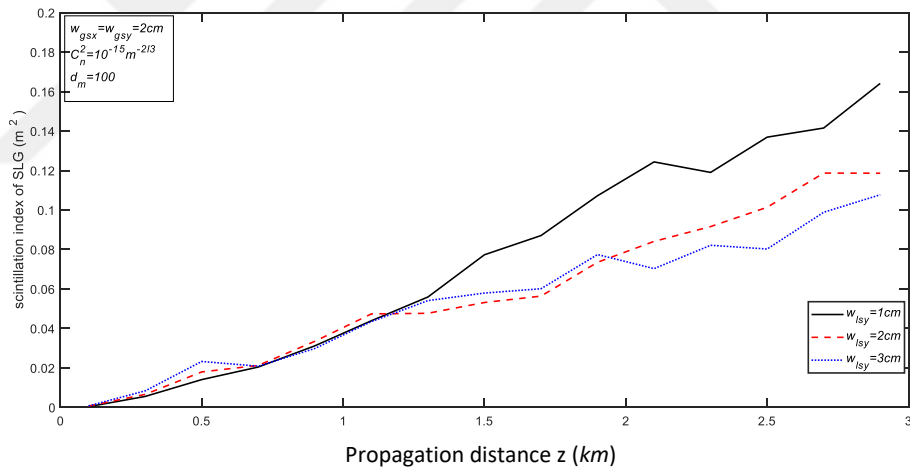
**Figure 34:** Aperture averaged scintillation curves against propagation distance at fixed aperture length with different source sizes of an  $SLG_{11}$  from random phase screen setup for  $d_m = 100$ ,  $C_n^2 = 10^{-15} m^{-2/3}$



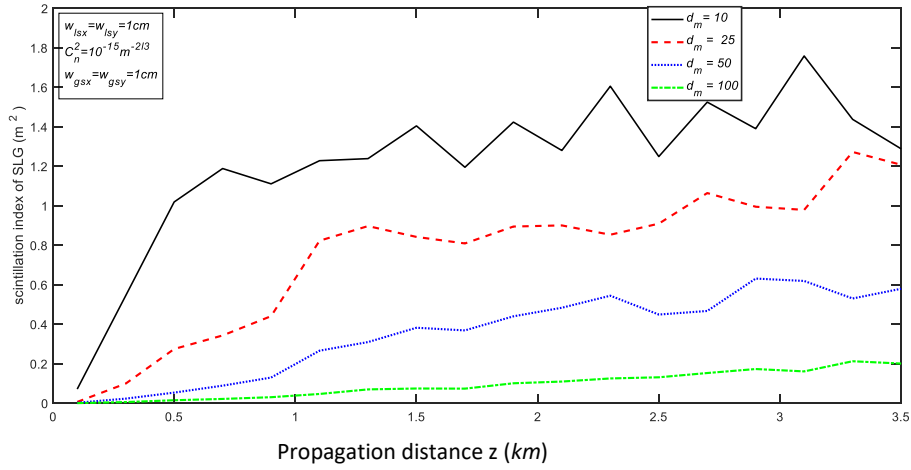
**Figure 35:** Comparison of point-like scintillation index curves from random phase screen setup for different wavelength of an  $SLG_{11}$  for  $d_m = 10$



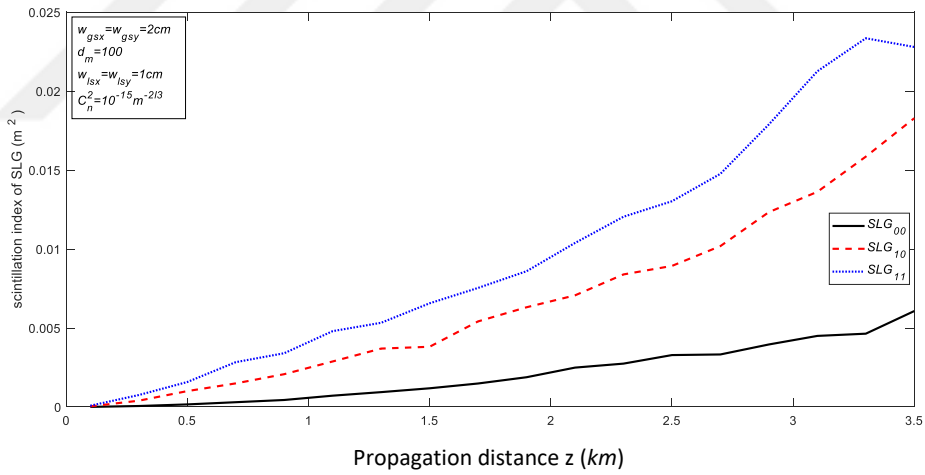
**Figure 36:** Aperture averaged scintillation curves against propagation distance at fixed aperture length with different source size of an  $SLG_{10}$  from random phase screen setup for  $d_m = 100$ ,  $C_n^2 = 5 \times 10^{-16} m^{-2/3}$



**Figure 37:** Aperture averaged scintillation curves against propagation distance at fixed aperture length with different source size of an  $SLG_{10}$  from random phase screen setup for  $d_m = 100$ ,  $C_n^2 = 10^{-15} m^{-2/3}$



**Figure 38:** Variation of scintillation curves against propagation distance at fixed aperture length with different  $d_m$  (side length of square aperture) of an  $SLG_{10}$  from random phase screen setup



**Figure 39:** Aperture averaged scintillation curves against propagation distance at fixed aperture length with different SLG beam order from random phase screen setup for  $d_m = 100$ ,  $C_n^2 = 10^{-15} m^{-2/3}$

## CHAPTER V

### Conclusion and Future Scope

#### 5.1 Conclusion

In this dissertation, the effect of atmospheric turbulence of a single beam type on the space system communications has been studied. A Super Lorentz Gaussian (SLG) beam of weak and moderate fluctuations is examined. So as to obtain the best shape of the beam at far propagation distance, the effect of the source sizes, wavelengths, beam orders are investigated. We presented a detailed comparison between different beam orders of SLG based on the point-like and power scintillations indices. Results of lowest scintillation index are obtained at larger propagation distance and smaller source size. Furthermore, we observed that the beam order  $(m, n)$  is a critical parameter for calculating the scintillation index of the standard Gaussian and the Super Lorentz Gaussian beams. Results of intensity patterns in the source plane are obtained based on the theoretical formulation of SLG beam and are compared with the existing formulations in the literature, then we have found these results in agreement. The scintillation patterns are obtained at the receiver plane of the horizontal path in the atmospheric links. The performance of the power scintillation of the focused SLG beam is explored with a finite-sized aperture in atmospheric turbulence. The scintillation index of the lowest order SLG beam (Gaussian beam) and the Gaussian beam of the scintillation index in the literature survey is compared under different parameters of the turbulence.

## 5.2 Future Scope

The results will be improved in the future and applied in a practical system which is used in optical communication at a long propagation distance based on slant path as shown.

- a. There is a scope to investigate the transmission of Super Lorentz-Gaussian beam SLG for different beam order in slant path.
- b. The properties of SLG beam and comparison with another beam can be studied in turbulent atmosphere for the case of slant path.
- c. The properties of SLG and Hermit-Gaussian beams can be investigated in anisotropic media for the case of turbulent atmosphere.
- d. The approach used in this work can be extended in the field of photonics.

## REFERENCES

- [1] Eyyubođlu H. T., Baykal Y., (2007), “*Scintillation Characteristics of Cosh-Gaussian beams*”, Appl. Opt., vol. 46, pp. 1099 -1106.
- [2] Lutomirski R. F and Yura H. T., (1969), “*Aperture-Averaging Factor of A Fluctuating Light Signal*”, J.Opt. Soc. Am., vol. 59, no. 9, pp.1247-1248.
- [3] Wang SJ., Baykal Y., Plonus MA., (1983), “*Receiver-Aperture Averaging Effects for the Intensity Fluctuation of A beam Wave in the Turbulent Atmosphere*”, J. Opt. Soc. Am., vol. 73, no. 6, pp. 831- 837.
- [4] Aarthi G., Prabu K., Reddy GR., (2017), “*Aperture Averaging Effects on The Average Spectral Efficiency of FSO Links over Turbulence Channel With Pointing Errors*”, Opt. Commun., vol. 385, pp. 136 -142.
- [5] Khalighi M. A., Uysal M., (2014)., “*Survey on Free Space Optical Communication: A Communication Theory Perspective*”, IEEE Commun. Surverys Tuts., vol.16, no. 4, pp. 2231- 2258.
- [6] Rayleigh Lord., (2010), “*X. On The Electromagnetic Theory of Light*”, Phil. Mag. S. 5., vol.12, no.73, pp. 81-101.
- [7] Wu H., Kavehrad M., (2007), “*Second Availability Evaluation of Ground-to-Air Hybrid FSO/RF Links*”, Int. J. Wireless Inf. Networks, vol. 14, no. 1, pp. 33 - 45.
- [8] Kouyoumjian R. G., (1965), “*Asymptotic high-frequency methods*”, in Proceedings of the IEEE. vol. 53, no. 8, pp. 864 - 876.

- [9] **Wait J. R., (1959)**, “*Electromagnetic Radiation from Cylindrical Structures*”, New York, pergamon press.
- [10] **Lawrence D., Sarabandi E. K., (2001)**, “*Electromagnetic Scattering from A Dielectric Cylinder Buried Beneath A Slightly Rough Surface*”, IEEE Trans Antennas and Propagation, vol. 4, no. 10, pp. 348 - 351.
- [11] **Borghi R., Frezza F., Schettini G., Gori F., Santarsiero M., (1996)**, “*Plane Wave Scattering by A Perfectly Conducting Circular Cylinder Near A Plane Surface: Cylindrical-Wave Approach*”, J. Opt. Soc. Am. A., vol. 13, no.3, pp. 483 - 493.
- [12] **Buyukaksoy A., Uzgoren G., (1988)**, “*Diffraction of High Frequency Waves by A Cylindrically Curved Surface with Different Face Impedance*”, IEEE Trans Antennas and Propagation, vol. 36, no. 5, pp. 592 - 600.
- [13] **Michaeli A., (1993)**, “*Application of Physical Optics and Physical Theory of Diffraction to A Smooth Convex Surface*”, J. Electromagnetic Waves App., vol. 7, no. 12, pp. 1623 - 1631.
- [14] **Syed H. H., Volakis J. L., (1996)**, “*PTD Analysis of Impedance Structures*”, IEEE Trans Antennas and Propagation, vol. 44, no. 7, pp. 983-988.
- [15] **Başdemir H. D., (2010)**, “*M.Sc. Thesis*”, Dept. of Elec. Comm. Eng., Çankaya Univ., Turkey.
- [16] **DE Bruin H. A. R., VAN DEN HURK B. J. J. M., Kohsiek W.,(1995)**, “*The Scintillation Method Tested over A Dry Vineyard Area*”, Boundary-Layer Meteorol, vol. 76, no. 1-2, pp. 25 - 40.
- [17] **Andrews L. C., Phillips RL., Hopen CY., Al-Habash MA.,(1999)**, “*Theory of Optical Scintillation*” , J. Opt. Soc. Am. A., vol. 16, no. 6, pp. 1417-1429.



- [18] **Andrews L. C., Al-Habash M. A., Hopen C. Y., Phillips RL., (2001)**, “*Theory of Optical Scintillation: Gaussian-beam Wave Model*” , *Waves Random Media.*, vol. 11, no. 3, pp. 271 - 291.
- [19] **Banakh V. A., Mironov V. L., (1978)**, “*Influence of the Diffraction Size of the Transmitting Aperture and of the Turbulence Spectrum on the Intensity Fluctuations of Laser Radiation*”, *Sov. J. Quantum Electronics*, vol. 8, no. 7, pp. 875 - 878.
- [20] **Miller W. B., Ricklin J. C., Andrews L. C., (1994)**, “*Effects of The Refractive Index Spectral Model on the Irradiance Variance of A Gaussian beam*”, *J. Opt. Soc. Am. A.*, vol. 11, no. 10, pp. 2719 - 2726.
- [21] **Patrushev G. Y., (1978)**, “*Fluctuations of the Field of A Wave beam on Reflection in A Turbulent Atmosphere*” , *Sov. J. Quantum Electronics*, vol. 8, no. 11, pp 1315 - 1318.
- [22] **Fante R. L., (1976)**, “*Comparison of Theories for Intensity Fluctuations in Strong Turbulence*” , *Radio Sci.*, vol. 11, no. 3, pp. 215 - 219.
- [23] **Gochelashvili K. S., Pevgov V. G., Shishov V. I., (1974)**, “*Saturation of Fluctuations of The Intensity of Laser Radiation at Large Distances in A Turbulent Atmosphere*”, *Sov. J. Quantum Electronics*, vol. 4, no. 5, pp. 632 - 637.
- [24] **Eyyuboğlu H. T., Baykal Yahya., Cai Yangjian., (2007)**, “*Complex Degree of Coherence for Partially Coherent General beams in Atmospheric Turbulence*” , *J. Opt. Soc. Am. A.*, vol. 24, no. 9, pp. 2891- 2901.
- [25] **Belousov S. I., Yakushkin I. G., (1980)**, “*Strong Fluctuations of Fields of Optical beams in Randomly Inhomogeneous Media*”, *Sov. J. Quantum Electronics*, vol. 10, no. 3, pp. 301-304.

- [26] Fleck J. A., Morris J. R., Feit M. D., (1978), “*Time-dependent propagation of high-energy laser beams through the atmosphere: II,*” Appl. Phys., vol. 14, no. 1, pp. 99- 115.
- [27] Banakh V. A., Krekov G. M., Mironov V. L., Khmelevtsov S. S., Tsvik R. Sh., (1974), “*Focused-Laser-beam Scintillations in the Turbulent Atmosphere,*” J. Opt. Soc. Am., vol. 64, no. 4, pp 516 - 518.
- [28] Vetelino F. S., Young C., Andrews L. C., Grant K., Corbett K., Clare B., (2005), “*Scintillation: Theory vs. Experiment* ”, in Proc. SPIE, vol. 5793, pp. 166 - 177.
- [29] Ricklin J. C., Davidson F. M., (2003), “*Atmospheric Optical Communication With A Gaussian–Schell beam*” , J. Opt. Soc. Am. A., vol. 20, no. 5, pp. 856 - 866.
- [30] Korotkova O., (2006), “*Control of the Intensity Fluctuations of Random Electromagnetic beams on Propagation in Weak Atmospheric Turbulence in Free-Space Laser Communication Technologies*”, in Proc. SPIE, Free-Space Laser Commun. Technol. XVIII, vol. 6105, pp. 54 - 64.
- [31] Tatarski V. I., (1961), “*Wave Propagation in A Turbulent Medium*”, McGraw-Hill Inc., New York.
- [32] Eyyuboğlu H. T., 2014, “*Notes on the use of Angular Spectrum Model and Random Phase Screen*”, [Online]. Available:  
[http://ece646.cankaya.edu.tr/uploads/files/ECE%20646\\_Notes%20on%20Angular%20Spectrum%20and%20RPS\\_HTE\\_Bahar%202014.pdf](http://ece646.cankaya.edu.tr/uploads/files/ECE%20646_Notes%20on%20Angular%20Spectrum%20and%20RPS_HTE_Bahar%202014.pdf), Last access : 29.09.2017.

- [33] **Arpali S. A., Baykal Y., (2009)**, “*Bit Error Rates for Focused General-type beams*”, Progress in Electromagnetics Research Symposium (PIERS), vol. 5, no. 7, pp. 633-636.
- [34] **Andrews L. C., Phillips R. L., (1998)**, “*Laser beam Propagation through Random Media*”, SPIE Press, Washington.
- [35] **Vetelino F. S., Andrews L. C., Voelz D. G., Ricklin J. C., (2004)**, “*Annular Gaussian beams in Turbulent Media, in Free-Space Laser communication and Active Laser Illumination III*”, in Proc. SPIE, Free-Space Laser Commun. and Active Laser Illumination III, vol. 5160, pp. 86 - 97.
- [36] **Feizulin Z. I., Kravtsov Y., (1967)**, “*Broadening of A Laser beam in A Turbulent Medium*”, Radiophys Quantum Electron., vol. 10, no. 1, pp 33-35.
- [37] **Wang S. C. H., Plonus M. A., (1979)** “*Optical beam propagation for A Partially Coherent Source in the Turbulent Atmosphere*”, J. Opt. Soc. Am., vol. 69, no. 9, pp. 1297-1304.
- [38] **Young C. Y., Gilchrest Y. V., Macon B. R., (2002)**, “*Turbulence Induced beam Spreading of Higher Order Mode Optical Waves*”, Opt. Eng., vol. 41, no. 5, pp. 1097 - 1103.
- [39] **Eyyuboğlu H. T., Baykal Y., (2005)**, “*Average Intensity and Spreading of Cosh-Gaussian Laser beams in the Turbulent Atmosphere*”, Appl. Opt., vol. 44, no. 6, pp. 976 - 983.
- [40] **Eyyuboğlu H. T., Baykal Y., (2004)**, “*Analysis of Reciprocity of Cos-Gaussian and Cosh-Gaussian Laser beams in Turbulent Atmosphere*”, Opt. Express., vol. 12, no. 20, pp. 4659 - 4674.

- [41] Eyyuboğlu H. T., Baykal Y., (2005), “*Hermit-Sine-Gaussian A Hermit-Sinh-Gaussian Laser beams in Turbulent Atmosphere,*” J. Opt. Soc. Am. A., vol. 22, no. 12, pp. 2709 - 2718.
- [42] Cai Y., He S., (2006), “*Average Intensity and Spreading of An Elliptical Gaussian beam in A Turbulent Atmosphere*” , Opt. Lett., vol. 31, no. 5, pp. 568-570.
- [43] Dou Lingyu., Ji Xiaoling., Li Peiyun., (2012), “*Propagation of partially coherent annular beams with decentered field in turbulence along a slant path*” , Opt. Express, vol. 20, no. 8, pp. 8417-8430.
- [44] Gawhary O.E., Severini S., (2006), “*Lorentz beams*”, J. Opt. A: Pure Appl. Opt., vol. 8, pp. 406 - 414.
- [45] Eyyuboğlu H. T., Arpali Ç., Baykal Y., (2006), “*Flat Topped beams and their Characteristics in Turbulent Media*”, Opt. Express, vol. 14, no. 10, pp. 4196 - 4207.
- [46] Eyyuboğlu H. T., Altay S., Baykal Y., (2006), “*Propagation Characteristics of Higher-Order Annular Gaussian beams in Atmospheric Turbulence*”, Opt. Commun., vol. 264, no. 1, pp. 25-34.
- [47] Jisha C. P., Alberucci A., (2017), “*Paraxial light beams in structured anisotropic media*”, J. Opt. Soc. Am. A., vol. 34, no. 11, pp. 2019-2024.
- [48] Eyyuboğlu H. T., Baykal Y., Ji X., (2010), “*Scintillations of Laguerre Gaussian beams*”, Appl. Phys. B., vol. 98, no. 4, pp. 857 - 863.
- [49] Gu Y., (2013), “*Statistics of Optical Vortex Wander on Propagation through Atmospheric Turbulence*”, J. Opt. Soc. Am. A., vol. 30, no. 4, pp. 708 - 716.

- [50] **Bissonnette L. R., (1977)**, “*Atmospheric scintillation of optical and infrared waves: a laboratory simulation*”, *Appl. Opt.*, vol. 16, no. 8, pp. 2242 - 2252.
- [51] **Shchepakina E., Korotkova O., (2010)**, “*Second-Order Statistics of Stochastic Electromagnetic beams Propagating through Non-Kolmogorov Turbulence*”, *Opt. Express.*, vol. 18, no. 10, pp. 10650 - 10658.
- [52] **Toselli I., Andrews L.C., Phillips R.L., Ferrero V., (2008)**, “*Free -Space Optical System Performance for Laser beam Propagation through Non-Kolmogorov Turbulence*”, *Opt. Eng.* vol. no. 47, pp. 26 -31.
- [53] **Toselli I., Andrews L.C., Phillips R.L., Ferrero V., (2009)**, “*Free Space Optical System Performance for A Gaussian beam Propagating through Non-Kolmogorov Weak Turbulence*”, *IEEE Trans Antennas and Propagation*, vol. 57, no. 6, pp. 1783 - 1788.
- [54] **Andrews L. C., Phillips R. L., Hopen C. Y.,(2001)**, “*Laser beam Scintillation with Applications*”, SPIE Press., Washington.
- [55] **Kedar D., Arnon S., (2004)**, “*Urban Optical Wireless Communication Networks: the Main Challenges and Possible Solutions*”, *IEEE Commun. Mag.*, vol. 42, no. 5, pp. 2-7.
- [56] **Peppas K. P., Mathiopoulos P. T., (2015)**, “*Free-Space Optical ommunication With Spatial Modulation and Coherent Detection Over H-K Atmospheric Turbulence Channels*”, *J. Lightw. Technol.*, vol. 33, no. 20, pp. 4221-4232.
- [57] **Haas S. M., (2003)**,“ *Ph.D. Dissertation*”, Massachusetts Institute of Technology,USA.

- [58] **Lee E. J., Chan V., (2004)**, “*Part 1: Optical Communication over the Clear Turbulent Atmospheric Channel Using Diversity*”, IEEE Journal on Selected Areas in Commun., vol. 22, no. 9, pp. 1896 -1906.
- [59] **Wilson S. G., Brandt-Pearce, Q M., Cao., Baedke M.,(2005)**, “*Optical Repetition MIMO Transmission with Multipoles PPM* ”, IEEE Journal on Selected Areas in Commun., vol. 23, no. 9, p.1901-1909.
- [60] **Navidpour S. M., Uysal M., Kavehrad M., (2007)**, “*BER Performance of Free-Space Optical Transmission with Spatial Diversity*”, IEEE Trans. Wireless Commun., vol. 6, no. 8, p. 2813 - 2819.
- [61] **Safari M., Uysal M., (2008)**, “*Do We Really Need OSTBC for Free Space Optical Communication with Direct Detection*”, IEEE Trans. Wireless Commun., vol. 7, no. 11, pp. 4445 - 4448.
- [62] **Karagiannidis G. K., Tsiftsis T. A., Sandalidis H. G.,(2006)**, “*Outage Probability of Relayed Free Space Optical Communication Systems*” , IEEE Electron. Lett., vol. 42, no. 17, pp. 994 - 995.
- [63] **Safari M., Uysal M., (2007),,** “*Relay-Assisted Free-Space Optical Communication*”, IEEE Trans. Wireless Commun.,vol. 7, no. 12, pp. 5441 - 5449.
- [64] **Safari M., Uysal M., Zhang K., (2008)**, “*Cooperative Diversity over Log-Normal Fading Channels Performance Analysis and Optimization*”, IEEE Trans. Wireless Commun., vol. 7, no. 5, pp. 1963 - 1972.
- [65] **Gori F., (1994)**, “*Flattened Gaussian beams,*” Opt. Coummun., vol. 107, no. 5, pp. 335-341.

- [66] **Alavinejad M., Ghafary B., Kashani F. D., (2007)**, “*Analysis of the Propagation of Flat-Topped beam with Various beam Orders through Turbulent Atmosphere*”, Optics and Lasers in Engineering, vol. 46, no. 1, pp. 1 - 5.
- [67] **Chen X., Ji X., (2008)**, “*Directionality of Partially Coherent Annular Flat-Topped beams Propagating through Atmospheric Turbulence*”, Opt. Commun., vol. 18, no. 15, pp. 4765 - 4770.
- [68] **Zhang JZ., Li YK., (2005)**, “*Atmospherically Turbulent Effects on Partially Coherent Flat-Topped Gaussian beam*”, in Proc. SPIE, vol. 5832, pp.48 - 55.
- [69] **Baykal Y., (2004)**, “*Correlation and Structure Functions of Hermite-Sinusoidal-Gaussian Laser beams in A Turbulent Atmosphere*”, J. Opt. Soc. Am., A., vol. 21, no. 7, pp. 1290 - 1299.
- [70] **Cai Y., (2006)**, “*Propagation of Various Flat-Topped beams in A Turbulent Atmosphere*”, J. Opt. A: Pure Appl. Opt., vol. 8, no. 6, pp. 537- 545.
- [71] **Gerçekcioğlu H., Baykal Y., (2011)**, “*Scintillation index of Flat-Topped Gaussian Laser beam in Strongly Turbulent Medium*”, J. Opt. Soc. Am., A., vol. 28, no., pp. 1540 - 1544.
- [72] **Gerçekcioğlu H., Baykal Y., (2013)**, “*BER of Annular and Flat-Topped beams in Non-Kolmogorov Weak Turbulence*”, Opt. Commun., vol. 286, no. 128, pp. 30-33.
- [73] **Zhu X., Kahn M., (2002)**, “*Free-Space Optical Communication through Atmospheric Turbulence Channels*”, IEEE Trans Commun., vol. 50, no. 8, pp. 1293 -1300.

- [74] **Park C. Soon., (2004)**, “*Transmit Power Allocation for BER Performance Improvement in Multicarrier Systems*”, IEEE Trans. Commun., vol. 52, no. 10, pp. 1658 - 1663.
- [75] **Uysal M., Navidpour SM., Li J., (2004)**, “*Error Rate Performance of Coded Free-Space Optical Links over Strong Turbulence Channels*”, IEEE Commun. Lett., vol. 8, no. 10, pp. 635- 637.
- [76] **Weyrauch T., Vorontsov M. A., (2004)**, “*Free-Space Laser Communications with Adaptive Optics Atmospheric Compensation Experiments*”, J. Opt. Fiber. Commun. Rep. 1, pp.355 - 379.
- [77] **KRAVTSOV Y. A., (1992)**, *Propagation of Electromagnetic Waves through A Turbulent Atmosphere*”, Rep. Prog. Phys., vol. 55, no. 1, pp. 39.
- [78] **Xu G., Zhang X., Wei J., Fu X., (2004)**, “*Influence of Atmospheric Turbulence on FSO Link Performance*”, in Proc. SPIE., vol. 5281, pp. 1 - 8.
- [79] **Korotkova O., Andrews L. C., Phillips R. L., (2004)**, “*Model for A Partially Coherent Gaussian beam in Atmospheric Turbulence with Application in Lasercom*”, Opt. Eng., vol. 43, no. 22, pp.331- 341.
- [80] **Andrews L. C., Phillips R. L., Hopen C. Y.,(2011)**, “ *Analysis Of Fading in The Propagation Channel for the ORCA Laser Communication System*”, in Proc. SPIE, Atmospheric Propagation VIII., vol. no. 8038, pp. 1 - 11.
- [81] **Frehlich R .,(1987)**, “*Simulation of Laser Propagation in A Turbulent Atmosphere*”, Appl. Opt., vol. 39, no. 3, pp. 393 - 397.
- [82] **Bufton JL., Iyer RS., Taylor LS., (1977)**, “*Scintillation Statistics Caused by Atmospheric Turbulence and Speckle in Satellite Laser Ranging*”, Appl. Opt., vol. 16, no. 16, pp. 2408 - 2412.



- [83] **Goodman J. W., (1985)**, “*Statistical Optics*”, Wiley, New York.
- [84] **Labreyrie A., (1970)**, “*Attainment of Diffraction Limited Resolution in Large Telescopes by Fourier Analyzing Speckle Patterns in Star Images*”, *Astron. & Astrophys.*, vol. 6, pp. 85 - 87.
- [85] **Li Y., (2002)**, “*Light beam with Flat-Topped Profiles*”, *Opt. Lett.*, vol. 27, no. 12, pp. 1007-1009.
- [86] **Carter W.H., (1980)**, “*Spot Size and Divergence for Hermite Gaussian beams of any Order*”, *Appl. Opt.*, vol. 19, pp. 1027 - 1029.
- [87] **Saghafi S., Sheppard CJR., (1998)**, “*Near Field And Far Field of Hermite-Gaussian and Laguerre-Gaussian Modes*”, *J. mod. Optics*, vol. 45, no. 10, pp. 1999 - 2009.
- [88] **Phillips R.L., Andrews L.C. (1983)**, “*Spot size and divergence for Laguerre Gaussian beams of any order*”, *Appl. Opt.*, vol. 22, no. 5, pp. 643 - 644.
- [89] **McQueen C. A., Arlt J., Dholakia, K. (1999)**, “*An Experiment to Study Nondiffracting Light beam*”, *Am. J. Phys.*, vol. 67, no. 10, pp. 912-915.
- [90] **McQueen CA., Arlt J., Dholakia K., (1992)**, “*Nondiffracting X Waves-Exact Solutions to Free-Space Scalar Wave Equation and their Finite Aperture Realizations*”, *Am. J. Phys.*, vol. 39, no. 1, pp. 19 - 31.
- [91] **Zhang W., Kuzyk MG., (2006)**, “*Effect of A Thin Optical Kerr Medium on A Laguerre-Gaussian beam*”, *Appl. Phys. Lett.*, vol. 89, no. 10, pp. 101-103.
- [92] **CAI Y., HE S., (2006)**, “*Propagation of Various Dark Hollow beams in A Turbulent Atmosphere*”, *J. Opt. Soc. Am. A.*, vol. 14, no. 4, pp. 1353 - 1367.

- [93] FREEGARDE T., DHOLAKIA K., (2002), “*Cavity Enhanced Optical Bottle beam as a Mechanical Amplifier*”, Phys. Rev. A., vol. 66, no 013413, pp. 1 - 8.
- [94] Santarsiero M., Borghi R., (1999), “*Correspondence between Super-Gaussian and Flattened Gaussian beams*,” J. Opt. Soc. Am. A., vol. 16, no. 1, pp. 188-190.
- [95] Lu B., Luo S., Ji X., (2001), “*A further Comparative Study of Flattened Gaussian beams and Super-Gaussian beams*”, J. Mod. Optics., vol. 48, no. 2, pp. 371-377.
- [96] Liu Dajun., Yin Hongming., Wang Guiqiu., Wang Yaochuan., (2017), “*Propagation of partially coherent Lorentz–Gauss vortex beam through oceanic turbulence*”, Appl. Opt., vol. 56, no. 31, pp. 8785-8792.
- [97] Zhou G., Zheng J., Xu Y., (2008), “*Investigation in the Far Field Characteristics of Lorentz beam from the Vectorial Structure*”, J. Mod. Optics., vol 55, no. 6, pp. 993 – 1002.
- [98] Zhou P., Wang X., Ma Y., Ma H., Xu X., Liu Z., (2010) , “*Average intensity and Spreading of A Lorentz beam Propagating in A Turbulent Atmosphere*”, J. Optics., vol. 12, no. 1, pp. 120 - 129.
- [99] Zhou G., (2009), “*Nonparaxial Propagation of A Lorentz–Gauss beam*”, J. Opt. Soc. Am. B., vol. 26, no. 1, pp. 141-147.
- [100] Zhou G., (2010), “*Propagation of A Partially Coherent Lorentz-Gauss beam through A Paraxial ABCD Optical System*”, Opt. Express., vol. 18, no. 5, pp. 4637- 4643.

- [101] **Indebetouw Guy., (2007)**, “*Optical Vortices and Their Propagation*”, J. Mod. Optics., vol. 40, no. 1, pp. 73 - 87.
- [102] **Flores-Arias. T., Díaz Rio A del., Bao-Varela C, M V Pérez., Gómez-Reino C., (2009)**, “*Description of gradient-index human eye by a first-order optical system*”, Appl. Phys. B., vol. 11, no 12. pp. 125301.
- [103] **Zhou G., (2009)**, “*Zn O Nanostructures for Dye-Sensitized Solar Cells*”, Appl. Phys. B., vol. 21, no. 41, pp. 4065-4184.
- [104] **Zhou G., (2009)**, “*The beam Propagation Factors and the Kurtosis Parameters of A Lorentz beam*”, Opt. Laser Technol., vol. 41, no. 8, pp. 953 - 955.
- [105] **Eyyuboğlu H. T., Sermutlu E., (2010)**, “*Calculation of Average Intensity via Semi-Analytic Method*”, Appl. Phys. B., vol. 98, no. 4, pp. 865 - 870.
- [106] **Doty S., Leung D., LEUNG M., (1994)**, “*A Critical Evaluation of Semianalytic Methods in the Study of Centrally Heated, Unresolved, Infrared Sources*”, APJ., vol. 424, no. 2, p. 729-747.
- [107] **Gawhary O.E., Severini S., (2007)**, “*Lorentz beams as a Basis for A New Class of Rectangularly Symmetric Optical Fields*” Opt. Commun. vol. 269, no. 2, pp. 274 - 284.
- [108] **Zhou G., (2010)**, “*Super Lorentz–Gauss Modes and their Paraxial Propagation Properties*”, J. Opt. Soc. Am. A., vol. 27, no. 3, pp. 563-571.
- [109] **Chen Ziyang., Pu Jixiong., (2007)**, “*Propagation characteristics of aberrant stochastic electromagnetic beams in a turbulent atmosphere*” J. Opt. A: Pure Appl. Opt., vol. 9, no. 12, pp. 1123-1130.

- [110] Eyyuboğlu H. T., (2011), “*Partially Coherent Lorentz Gaussian beam and its Scintillations*”, Appl. Phys. B., vol. 103, no. 3, pp. 755 - 762.
- [111] Godson W. L., (1953), “*The Evaluation of Infra-Red Radiative Fluxes due to Atmospheric Water Vapour*”, Quarterly Journal of the RMetS., vol. 79, no. 341, pp. 367-379.
- [112] Schmidt P.P., (1976), “*A Method for the Convolution of Line Shapes which Involve the Lorentz Distribution*”, J. Physics B., vol. 9, no. 13, pp. 2331 - 2339.
- [113] Arpali Ç., Yazicioğlu C., Eyyuboğlu H. T., (2006), “*Simulator for General-Type beam Propagation in Turbulent Atmosphere*”, Opt. Express., vol. 14, no. 20, pp. 8918 - 8928.
- [114] Shirai T., Dogariu A., Wolf Emil., (2003), “*Mode Analysis of Spreading of Partially Coherent beams Propagating through Atmospheric Turbulence*”, J. Opt. Soc. Am. A., vol. 20, no. 6, pp. 1094 -1102.
- [115] Mahdiah M. H., (2008), “*Numerical Approach to Laser beam Propagation through Turbulent Atmosphere and Evaluation of beam Quality Factor*”, Opt. Commun., vol. 281, no. 13, pp. 3395-3402.
- [116] Gökçe M. C.,(2012), “*Ph.D. Dissertation*”, Dept. of Elec. Comm. Eng., Çankaya Univ., Turkey.
- [117] Lukin V. P., Pokasov V. V.,(1981), “*Optical Wave Phase Fluctuations* ” Appl. Opt., vol. 20, no. 1, pp. 121-135.
- [118] Khamees H. T., (2018), “*Power Scintillation for SLG Beam Evaluation by Using A Random Phase Screen Method*”, Ciência e Técnica Vitivinícola.



## CURRICULUM VITAE



### PERSONAL INFORMATION

**Surname, Name:** Hussein Thary Khamees AL-GRAIRI

**Date and Place of Birth:** 26 Feb 1963, Baghdad

**Marital Status:** Married

**Phone:** +964 770 268 5531

**Email:** husenthary@gmail.com

### EDUCATION

Degree	Institution	Year of Graduation
M.Sc.	University of Technology, Baghdad	2004
B.Sc.	Al-Mustenseria University, Baghdad	1996
High School	Al-Kathomyia Secondary, Baghdad	1981

### WORK EXPERIENCE

Year	Place	Enrollment
1983	Organization of Research	Official work
2006	Ministry of Higher Education	Lecturer
<b>Foreign Languages</b>	Advanced English, Arabic Native	Turkish
<b>HOBBIES</b>	Kick Boxing, Travel, Books,	Swimming, Fitness